Prefoldin protects neuronal cells from polyglutamine toxicity by preventing aggregation formation*

Erika Tashiro[1,2], Tamotsu Zako[3], Hideki Muto[4], Yoshinori Itoo[3,5], Karin Sörgjerd[3], Naofumi Terada[4], Akira Abe[1,2], Makoto Miyazawa[1,2], Akira Kitamura[4], Hirotake Kitaura[1], Hiroshi Kubota[6], Mizuo Maeda[3], Takashi Momoi[7], Sanae M.M. Iguchi-Ariga[8] Masataka Kinjo[4], and Hiroyoshi Ariga[1,]

From the Graduate School of Pharmaceutical Sciences, Hokkaido University, Sapporo 060-0812, Japan[1], the Graduate School of Life Science, Hokkaido University, Sapporo 060-0810, Japan[2], the Bioengineering Laboratory, RIKEN Institute, 2-1 Hirosawa, Wako 351-0106, Saitama, Japan[3], the Laboratory of Molecular Cell Dynamics, Faculty of Advanced Life Science, Hokkaido University, Sapporo 001-0021, Japan[4], the School of Frontier Sciences, The University of Tokyo, Kashiwa 277-0000, Chiba Japan[5], the Graduate School and Faculty of Engineering and Resource Science, Akita University, Akita 010-8502, Japan[6], the Center for the Medical Research, International University of Health and Welfare, 2600-1 Kitakanemaru, Otawara 324-0011, Tochigi, Japan[7], and the Graduate School of Agriculture, Hokkaido University, Kita-ku, Sapporo 060-8589, Japan[8]

*Running title: Inhibition of polyglutamine toxicity by prefoldin

To whom correspondence should be addressed: Hiroyoshi Ariga, Graduate School of Pharmaceutical Sciences, Hokkaido University, Kita-ku, Sapporo 060-0812, Japan. Tel.: +81 11 706 3745; Fax: 81 11 706 4988; E-mail: hiro@pharm.hokudai.ac.jp

Key words: prefoldin; chaperone; Huntington disease; protein aggregation; cell death

Backgrounds: Prefoldin, a molecular chaperone comprised of six subunits, prevents misfolding of newly synthesized nascent polypeptides.

Results: Prefoldin inhibited aggregation of pathogenic Huntingtin and subsequent cell death.

Conclusion: Prefoldin suppressed Huntingtin aggregation at the small oligomer stage.

Significance: Prefoldin plays a role in preventing protein aggregation in Huntington disease.

ABSTRACT

Huntington disease is caused by cell death after the expansion of polyglutamine (polyQ) tracts longer than approximately 40 repeats encoded by exon 1 of the *huntingtin* (Htt) gene. Prefoldin is a molecular chaperone comprised of six subunits, PFD1~6, and prevents misfolding of newly synthesized nascent

polypeptides. In this study, we found that knockdown of PFD2 and PFD5 disrupted prefoldin formation in Htt-expressing cells, resulting in accumulation of aggregates of a pathogenic form of Htt and in induction of cell death. Dead cells, however, did not contain inclusions of Htt, and analysis by a fluorescence correlation spectroscopy indicated that knockdown of PFD2 and PFD5 also increased the size of soluble oligomers of pathogenic Htt in cells. *In vitro* single molecule observation demonstrated that prefoldin suppressed Htt aggregation at the small oligomer (dimer to tetramer) stage. These results indicate that prefoldin inhibits elongation of large oligomers of pathogenic Htt, thereby inhibiting subsequent inclusion formation, and suggest that soluble oligomers of polyQ-expanded Htt are more toxic than are inclusion to cells.

INTRODUCTION

Huntington disease (HD) is a progressive neurodegenerative disorder characterized by motor impairment, involuntary movements (chorea), psychiatric disorders and dementia (1). HD is caused by the expansion of a CAG repeat in exon 1 of the *huntingtin* gene, and resultant polyglutamine (polyQ) tracts longer than approximately 40 repeats trigger cell death of affected neurons (2, 3). The conformation of huntingtin (Htt) protein is altered by the existence of expanded polyQ, leading to oligomerization and aggregation of mutant/pathogenic Htt into β-sheet-rich fibrils, thereby forming large aggregates (inclusion bodies) in affected neurons (4, 5). The monomer of pathogenic Htt protein is assumed to form a conformation rich in random coils or α-helices and to turn β-sheets (6, 7). Oligomerized pathogenic Htt, on the other hand, tends to form fibrils and inclusions. Although the inclusion body of pathogenic Htt have long been thought to be a causative factor for Huntington disease, accumulating evidences suggest that formation of pathogenic Htt inclusion is not correlated with neuronal cell death (8, 9). It is therefore thought that the inclusion body act as a deposit of pathogenic Htt to decrease the risk of neuronal cell death.

Many molecular chaperones associate with polyglutamine proteins to inhibit formation of aggregations in test tubes, cell lines and model animals (10-14). Purified heat shock proteins HSP70 and HSP40 (Hdj1) suppress the toxicity of polyQ-expanded Htt exon 1: These proteins promote formation of non-toxic oligomers of polyQ-expanded Htt, instead of SDS-insoluble amyloid fibrils (15, 16). Furthermore, several groups have reported that over-expression of Hsp70/Hsp40 chaperones suppresses polyQ-induced neurotoxicity in animal models of polyglutamine disease (17-19) and that chaperonin CCT (chaperonin-containing TCP-1, also known as TRiC) prevents the toxicity of pathogenic Htt by inhibiting formation of toxic oligomers through interaction with soluble oligomers (20-22). It is therefore possible that other chaperones also modify aggregation of

pathogenic Htt.

Prefoldin is a molecular chaperone found in eukarya and archaea domains and assists folding of a newly synthesized polypeptide chain in cooperation with Hsp70/Hsp40 and with CCT in the cytosol (23, 24). Prefoldin is comprised of six subunits, PFD1~6, and it forms a "jellyfish-like" structure (25) and binds to a substrate with its tentacle-like structures (26). Although distal end regions of prefoldin's tentacles are hydrophobic and are thought to be accessible with hydrophobic surfaces of the substrate (25), little is known about the mechanisms by which prefoldin recognizes substrates. Prefoldin binds to newly synthesized nascent polypeptides such as actin and tubulin in the cytosol to prevent their misfolding (24, 27). Recent studies have shown that capturing newly synthesized polypeptide chains, prefoldin transports them to CCT to assist folding of polypeptides (23, 24, 28). Furthermore, Sakono and coworkers have reported that archaeal prefoldin forms soluble amyloid β oligomers but not fibrils in vitro (29), suggesting that prefoldin plays a modifier role against the toxicity of misfolded proteins, including proteins that cause neurodegenerative diseases.

In this study, we examined the effect of human prefoldin on the formation and toxicity of pathogenic Htt aggregation using *in vitro* and *in vivo* systems and found that prefoldin prevents Htt neurotoxicity by inhibiting its aggregation at a small oligomer stage. We discuss prefoldin-dependent protection mechanisms of neuronal cells against the toxicity of pathogenic Htt.

EXPERIMENTAL PROCEDURES

Plasmids

pEGFP-C1 and pcDNA3 were obtained from Clontech (Mountain View, CA, USA) and Invitrogen (Carlsbad, CA, USA), respectively. Expression vectors for EGFP-Q11 and EGFP-Q72 and for Htt-exon 1 fused with GFP were described previously (21, 30). Htt-polyQ-GFP regions were recloned into ptet-CMVminimal containing minimal CMV promoter. pGEXGST-myc-Htt Q23/Q53 exon 1 (15, 31) were used for expression of GST-Htt proteins in *E. coli*. For fluorescence labeling of GST-Htt exon 1, all of the cysteine residues present in GST were replaced with serine as described previously (20).

Analyses of aggregate-containing cells and cell death

Neuroblastoma Neuro-2a cells were cultured in Dulbecco's modified Eagle's medium supplemented with 10% calf serum. Cells were cultured on a 3.5-cm glass bottom dish (Iwaki, Tokyo, Japan) coated with type IV collagen (Cellmatrix, Nitta Gelatin, Osaka, Japan). Nucleotide sequences of the upper and lower strands for siRNA were as follows: 5'-GGAGCAUGUGCUUAUUGAUGU-3' and 5'-AUCAAUAAGCACAUGCUCCAC-3' for PFD2, and 5'-GGAGCGGACUGUCAAAGAATT-3' and 5'-UUCUUUGACAGUCCGCUCCTT-3' for PFD5. Neuro-2a cells were first transfected with

PFD2 siRNA and PFD5 siRNA using Lipofectamine 2000 reagent (Invitrogen). Allstars Negative control siRNA (QIAGEN) was used as a non-specific negative control (Qiagen, Hilden, Germany). Twenty-four h after transfection, cells were transfected with 0.2 μg of an expression vector for EGFP-polyQ or Htt-polyQ-GFP and induced to undergo neuronal cell differentiation by addition of 5 mM dibutyryl cAMP for 48 h. After transfection of polyQ expression vectors into Neuro-2a cells, the medium was replaced with fresh medium containing 0 or 5 mM dibutyryl cAMP and 2 μg/ml propidium iodide. At 48 h after transfection, cell images were taken by using Biozero BZ-8000 (Keyence, Osaka, Japan) with Plan-Apo 20 x 0.75 NA (Nikon, Tokyo, Japan). Propidium iodide-positive cells were counted as dead cells.

Neuro-2a cells were transfected with 5 and 10 ng expression vectors for six prefoldin subunits PFD1-6 using Lipofectamine 2000 reagent. Twenty-four h after transfection, cells were transfected with an expression vector for Htt23-polyQ-GFP or Htt78-polyQ-GFP. Neuronal differentiation of Neuro-2a cells was then carried out as described above.

Western blotting

Proteins were extracted from cells after incubation of cells with a Hepes buffer containing 40 mM Hepes-NaOH (pH 7.4), 120 mM NaCl, 1 mM EDTA, 0.5% NP-40 and protease inhibitors and subjected to Western blot analysis with anti-PFD1 (PA006499, Sigma, St. Louis, MO, USA), anti-PFD2, anti-PFD3 (K-13, Santa Cruz, Santa Cruz, CA, USA), anti-PFD4, anti-PFD5 (S-20, Santa Cruz), anti-PFD6 (AP2836a, Abgent, San Diego, CA, USA) and anti-GAPDH (MAB374, Chemicon, Temecula, CA, USA) antibodies. Proteins were then reacted with an IRDye800- or Alexa Fluor 680-conjugated secondary antibody and visualized by using an infrared imaging system (Odyssey, LI-COR, Lincoln, NE, USA). Anti-PFD2 and anti-PFD4 antibodies were established by injection of GST-PFD2 and GST-PFD4, respectively, into rabbits. The anti-PFD2 antibody was purified from rabbit serum, and serum from GST-PFD4-injected rabbits was used as the anti-PFD4 antibody.

Glycerol density gradient centrifugation to separate the prefoldin complex

Neuro-2a cells in a 10-cm dish were transfected with 240 μmol siRNAs targeting PFD2 and PFD5 and with non-specific siRNA. At 48 h after transfection, proteins were extracted from cells in a Hepes buffer and separated by a glycerol density gradient centrifugation at 40,000 rpm for 16 h at 4°C using an SW41 rotor. After samples had been fractionated into 22 fractions, proteins in fractions were precipitated with acetone at -80°C for 1 h, dissolved in an SDS buffer containing 50 mM Tris-HCl (pH 6.8), 1% SDS, 2% β-mercaptoethanol and 8.7% glycerol, and subjected to Western blotting or CBB staining on 15% SDS-containing polyacrylamide gels. Aldolase (160 kDa), bovine serum albumin (BSA) (56 kDa) and RNase A (13 kDa) were used as

molecular weight markers. When differentiated Neuro-2a cells were used, proteins were separated on 7.5% SDS-containing polyacrylamide gels, and Native Mark (Invitrogen) was used as molecular weight markers.

Immunofluorescence microscopy

Neuro-2a cells were cultured on coverslips and transfected with an expression vector for Htt-polyQ-EGFP. At 48 h after transfection, cells were fixed with 4% paraformaldehyde in PBS at 37°C for 10 min for staining PFD2, PFD5 and GAPDH or with methanol at -20°C for 5 min for staining CCT and Hsc70. After treatment of cells with 0.5% Triton X-100 for 10 min, cells were incubated with a blocking buffer containing 5% calf serum, 20% glycerol and 0.02% Triton X-100 at 4°C for 16 h. Cells were stained with anti-PFD2 (1:100), anti-PFD5 (1:50), anti-Hsc70 (1:100, SPA-815, Stressgen, Farmingdale, NY, USA), anti-CCT (1:100, sc-47717, Santa Cruz) and anti-GFP (1:100, JL-8, MBL, Nagoya, Japan) antibodies and then reacted with Alexa Fluor 594-conjugated anti-rabbit, anti-rat or anti-mouse IgG antibody (1:100, Invitrogen). Images were observed using LSM510 META (Carl Zeiss, Jena, Germany) with Plan-Apo 63x/1.4 DIC. An anti-PFD5 antibody for immunofluorescence detection was developed by us after immunization of rabbits with recombinant GST-PFD5 and purified from serum through an affinity column with GST-PFD5.

Filter-trap assay of cell lysates

At 48 h after transfection, cells were lysed in PBS containing 1% Triton X-100 and protease inhibitors and sonicated using a water bath-type sonicator at 4°C for 5 min. Lysates were diluted with 1% SDS-PBS, boiled for 10 min, and filtrated through a cellulose acetate membrane (0.2 μm) using a dot blotter (Bio-dot SF, Bio-Rad, Hercules, CA, USA). The membrane was incubated with 5% skim milk in PBS overnight and reacted with a mouse anti-GFP antibody (JL-8). The membrane was then reacted with an Alexa Fluor 680-conjugated secondary antibody, and proteins on the membrane were visualized by an Odyssey system.

FCS analysis

At 48 h after transfection, cells were lysed in PBS containing 1% Triton-X100 and protease inhibitors, sonicated as described above, and centrifuged at 15,000 rpm for 10 min at 4°C to remove insoluble GFP-polyQ aggregates. Supernatants were then filtrated through a PVDF membrane (0.22 μm) and replaced on a glass bottom 96-well plate and then subjected to FCS analysis using a ConfoCor 2 system with a water immersion objective lens (C-Apochromat 40 x 1.2 NA, Carl Zeiss) at excitation of 488 nm and emission of 505-550 nm. The confocal pinhole diameter was adjusted to 70 μm and fluorescence was measured 50 times for 10 sec at room temperature. Analyses by FCS were performed as described previously (21).

Protein purification

GST-fused with Htt exon 1 (GST-Htt23Q and GST-Htt53Q) were expressed in *E. coli* (BL21DE3) and purified as described previously (32). Human prefoldin (hPFD) was assembled from six individual subunits of PFD that had been expressed in and purified from *E. coli* (BL21DE3) as described previously (33).

Filter trap assay of in vitro aggregation

Htt protein was prepared by digestion of GST-Htt with PreScission protease (GE Healthcare, Little Chalfont, UK) to cleave off GST and reacted with hPFD or with BSA as a negative control in a buffer A containing 50 mM sodium phosphate (pH 8.0), 150 mM NaCl, 1 mM EDTA at 30˚C for 13 h as described previously (15). Reaction mixtures were then filtrated through a cellulose acetate membrane using a dot blotter and washed three times with TBST (0.05% Tween 20 in TBS). After blocking the membrane with 5% skim milk in TBST, the membrane was incubated with a mouse anti-c-myc antibody (1:1000, 9E10, Santa Cruz) and then with a horseradish peroxidase-conjugated anti-mouse IgG antibody (1:2000, R&D Systems, Minneapolis, MN, USA). Proteins were visualized using an ECL Plus blotting detection system (GE Healthcare).

Electron microscopy

Htt protein samples were diluted 10-fold with distilled water and placed on a carbon-coated copper grid and air-dried. After negative staining of samples with uranyl acetate, images were taken with an excitation voltage of 100 kV using a JEM-1011 transmission electron microscope (JEOL, Tokyo, Japan).

TIRFM single particle analysis of aggregation

A unique cysteine residue on GST-HttQ23 or GST-HttQ53 was labeled with a 10-fold molar excess of Alexa Fluor 488-maleimide (Invitrogen) in a labeling buffer containing 50 mM sodium phosphate pH 8.0, 150 mM NaCl and 10% glycerol for 4 h at 4°C. Excess free dye was removed by a NAP5 column (GE Healthcare), and a typical ratio of GST-Htt:labeled dye was 1:0.7. After addition of PreScission protease to the mixture, Alexa Fluor 488-labeled GST-HttQ23/53 (2.5 μM) was incubated with hPFD (2.5 μM) at 30°C for 13 h. Samples were then diluted 3000-fold and analyzed by TIRFM (34-36). Alexa Fluor 488-labeled proteins were illuminated with a blue solid-state laser (11.8 mW, 488 nm, Coherent). The fluorescence emission from the specimen was collected with an oil-immersion microscope objective (1.40 NA, x100, PlanApo, Olympus, Tokyo, Japan), and images were taken using a CCD camera (MC681SPD-R0B0, Texas Instruments, Dallas, TX, USA) coupled with an image intensifier (C8600, Hamamatsu Photonics, Hamamatsu, Japan). Fluorescence intensity of the single dye was determined from a distribution of photobleaching unitary step intensities of labeled monomer proteins. The number of HttQ53 molecules per particle was estimated by dividing initial fluorescence intensities from the single particle by fluorescence intensity of the single dye (37).

Statistical analyses

Data are expressed as means ± S.D. Statistical analyses were performed using analysis of variance (one-way ANOVA) followed by unpaired Student's *t*-test. For comparison of multiple samples, the Tukey-Kramer test was used.

Ethics statement

All animal experiments were carried out in accordance with the National Institutes of Health Guide for the Care and Use of Laboratory Animals, and the protocols were approved by the Committee for Animal Research at Hokkaido University (the permit number 08-0467).

RESULTS

Knockdown of prefoldin subunits causes disruption of prefoldin complex.

The prefoldin complex is composed of six subunits (PFD1~6), and these subunits are divided into α-type and β-type subunits based on their secondary structures (25). To examine the role of prefoldin in polyQ/Htt aggregation, we used a siRNA-mediated knockdown system to reduce the expression of prefoldin subunits in cells. Since the prefoldin complex contains two α-type subunits (PFD3 and PFD5) and four β-type subunits (PFD1, PFD2, PFD4 and PFD6), siRNAs targeting PFD5 (α-type subunit) and PFD2 (β-type subunit) were chosen for knockdown. Synthetic PFD2 and PFD5 siRNAs were ectopically transfected into mouse neuroblastoma Neuro-2a cells, and the expression levels of PFD2 and PFD5 mRNAs were examined by RT-PCR. The results showed that PFD2 and PFD5 mRNA levels were specifically reduced by their own siRNAs (data not shown). Analysis of prefoldin subunits by Western blotting showed that protein levels of PFD2 and PFD5 in siRNA-transfected cells were decreased to approximately 25% and 15%, respectively, of those in non-specific siRNA-transfected cells (control) (Fig. 1A). In addition to reduced levels of PFD2 and PFD5, protein expression levels of other subunits were also reduced, though the levels of PFD2 and PFD3 were unaffected by PFD5 siRNA. These results support the notion that the expression levels of prefoldin subunits are mutually regulated at the protein level through the ubiquitin-proteasome system as we reported previously (38). To examine whether knockdown of a prefoldin subunit affects formation of the prefoldin complex, proteins extracted from siRNA-transfected cells were separated on a glycerol density gradient followed by Western blotting with anti-PFD2 and anti-PFD5 antibodies. The prefoldin complex was observed in fractions 8-14 by estimating the fractions compared to those of protein markers, aldolase (160 kDa), bovine serum albumin (BSA) (56 kDa) and RNase A (13 kDa), in the gradient. As shown in Fig. 1B, amounts of the prefoldin complex in cells that had been transfected with PFD2 and PFD5 siRNAs were reduced to 12% and 15%, respectively, of that in control cells, indicating that RNAi-mediated knockdown of PFD2 and PFD5 effectively reduced formation of the prefoldin complex. As we reported previously (38), these

results suggest that free forms of prefoldin subunits are unstable compared to prefoldin subunits in the prefoldin complex.

Knockdown of PFD2, but not that of PFD5, strongly stimulates polyQ/Htt aggregation in undifferentiated Neuro-2a cells.

Since the pathogenic length of expanded polyQ in Huntington disease patients is longer than approximately 40 repeats, polyQ tracts containing 11 and 72 repeats were fused with GFP at the N-terminus (GFP-Q11 and GFP-Q72) and used as non-pathogenic and pathogenic models, respectively. To examine the effect of prefoldin on polyQ aggregation under pathologically relevant conditions, exon 1 of the *huntingtin* gene encoding 23 and 78 repeats of glutamine was also fused with GFP at the C-terminus (HttQ23-GFP and HttQ78-GFP). Undifferentiated Neuro-2a cells were transfected with PFD2 siRNA, PFD5 siRNA or non-specific siRNA as a control. At 24 h after transfection, cells were transfected with expression vectors for GFP-polyQ and HttQ-GFP, and GFP signals in cells were analyzed using a fluorescence microscope at 48 h after transfection of GFP-polyQ and HttQ-GFP. As shown in Figs. 1C and 1D, PFD2 knockdown increased numbers of dots in GFP-Q72- and HttQ78-GFP-expressing cells but not in cells expressing GFP, GFP-Q11 or HttQ23-GFP. Dots are large protein aggregates and termed as inclusions. Although PFD5 knockdown also slightly but significantly increased GFP-Q72 aggregation, the degree of aggregation was less than that in the case of PFD2 knockdown, and no significant increase in aggregation of HttQ78-GFP was observed after cells had been knocked down by PFD5 siRNA. Filter-trap assays were also carried out to examine the effects of PFD2 and PFD5 knockdown on aggregation of polyQ and Htt. The results showed that PFD2 knockdown stimulated formation of SDS-insoluble aggregates of GFP-Q72 and HttQ78-GFP but that the effect of PFD5 knockdown was weak compared to that of PFD2 knockdown (Figs. 1E and 1F), being consistent with the results of microscopic observation. These results indicate that knockdown of PFD2 and that of PDF5, but to a lesser extent, increase aggregation of polyQ-expanded proteins in undifferentiated Neuro-2a cells.

Knockdown of PFD5 and PFD2 stimulates toxicity and aggregation of polyQ/Htt in differentiated Neuro-2a cells.

To examine the effect of prefoldin on the toxicity of polyQ-expanded proteins in differentiated neuronal cells, Neuro-2a cells were transfected with PFD2 siRNA, PFD5 siRNA or non-specific siRNA as a control. At 24 h after transfection, cells were transfected with expression vectors for healthy and pathogenic forms of GFP-polyQ and Htt-GFP, treated with 5 mM dibutyryl cyclic AMP (db-cAMP) at 4 h after transfection, and analyzed at 48 h after transfection of GFP-polyQ and Htt-GFP. It was first confirmed that PFD2 and PFD5 siRNAs effectively decreased expression levels of PFD subunits in differentiated Neuro-2a cells (Fig. 2A). The reduced level of the prefoldin

complex in differentiated Neuro-2a cells was also confirmed by glycerol gradient centrifugation (data not shown). Furthermore, as described in the Introduction section, various chaperones influence polyQ formation. It is therefore possible that knockdown of prefoldin affects the expression level of chaperones. The expression levels of HSP70, HSC70, HSP40, and CCTα in Neuro-2a cells that had been transfected with PFD2 siRNA, PFD5 siRNA or non-specific siRNA were examined by Western blotting. As shown in Fig. 2B, there are little or no change of their expression levels both in undifferentiated and differentiated cells. Microscopic observation of GFP-polyQ and Htt-GFP showed that aggregation of pathogenic forms, but not that of healthy forms, of GFP-polyQ and Htt-GFP was significantly enhanced by both knockdown of PFD5 and that of PFD2 (Figs. 2C-2E). Filter-trap assays also showed that knockdown of PFD5 and PFD2 increased the amount of SDS-insoluble aggregates of pathogenic forms of polyQ proteins in differentiated Neuro-2a cells (Figs. 2F and 2G).

Overexpression of prefoldin reduced aggregation of polyQ/Htt in differentiated Neuro-2a cells.

To examine the effect of prefoldin on aggregation of polyQ/Htt in differentiated Neuro-2a cells, Neuro-2a cells were first transfected with two doses of expression vectors for 6 prefoldin subunits or a control vector and then with those for HttQ23-GFP and HttQ78-GFP. Forty-eight h after transfection, the expression level of prefoldin and formation of the prefoldin complex in cells were examined by Western blotting and by a glycerol density gradient centrifugation followed by Western blotting, respectively, with anti-PFD2 and anti-PFD5 antibodies. As shown in Figs. 3A and 3B, the levels of expression and formation of prefoldin were increased in a dose-dependent manner. Filter-trap assays were then carried out using cell extracts from prefoldin and Htt-GFP-transfected cells. The results showed that overexpressed prefoldin reduced the level of aggregated form of HttQ78-GFP but not HttQ23-GFP in a dose-dependent manner (Fig. 3C).

Pathogenic Htt-induced cell death occurs in cells without inclusions.

Neuro-2a cells were transfected with PFD2 siRNA and PFD5 siRNA and then transfected with expression vectors for healthy and pathogenic forms of Htt-GFP and differentiated with db-cAMP as described above. At 48 h after transfection of Htt-GFP, cells expressing HttQ23-GFP and HttQ78-GFP (green) were stained with propidium iodide (PI), and dead cells (PI staining-positive cells) were counted. As shown in Figs. 4A and 4B, knockdown of PFD2 significantly increased pathogenic Htt-induced cell death in both undifferentiated and differentiated Neuro-2a cells, and PFD5 knockdown significantly stimulated pathogenic Htt-induced cell death only in differentiated Neuro-2a cells. The effects of PFD5 knockdown in differentiated Neuro-2a cells are in contrast to those in undifferentiated Neuro-2a cells in terms

of aggregate formation. These results suggest that prefoldin-dependent protective reactions against toxicity of polyQ-expanded proteins are stronger in differentiated neuronal cells than in undifferentiated cells.

To assess cell death induced by polyQ aggregation, the number of dead cells containing inclusions in cells shown in Figs. 4A and 4B was counted. As shown in Figs. 4C and 4D, more than 90% of both undifferentiated and differentiated forms of dead Neuro-2a cells contained diffusely distributed but not largely aggregated cytosolic HttQ78 (HttQ78 inclusion), but the number of HttQ78 inclusions in undifferentiated cells was slightly larger than that in differentiated cells, indicating that knockdown of PFD2 and PFD5 did not significantly affect the number of HttQ78 inclusions, These results suggest that protective activity of prefoldin against HttQ78-induced cell death occurs before inclusion formation and that protective activity is stronger in differentiated cells than in undifferentiated cells.

Since prefoldin inhibited cell death in an inclusion formation-independent manner, localization of prefoldin in HttQ78-GFP-expressing Neuro-2a cells was examined by immunofluorescence staining with anti-PFD2 and PFD5 antibodies. As shown in Fig. 4E, neither PFD2 nor PFD5 (red color) was co-localized with HttQ78-GFP inclusions (green color), and PFD2 and PFD5 were diffusely distributed in the cytosol (Figs. 4E-a and 4E-b). The distribution pattern of PFD2 and PFD5 was similar to that of CCT (Fig. 4E-c) but was different from that of HSC70, which was co-localized with HttQ78-GFP inclusions (Fig. 4E-d). These results suggest that prefoldin prevents formation of pathogenic Htt aggregates by interacting with monomers or soluble oligomers rather than with inclusions, as does CCT but not HSC70.

Size of Htt-soluble aggregates is increased by prefoldin knockdown.

Although the presence of Htt inclusions in the brain of Huntington disease patients is a hallmark of Huntington disease, studies showed that formation of Htt inclusions was not correlated with the degree of cell death, suggesting that polyQ/Htt oligomers, rather than inclusions, are toxic to neurons (8, 9). We therefore examined whether prefoldin affects soluble oligomer formation of pathogenic Htt by using fluorescence correlation spectroscopy (FCS). FCS is a tool for investigating dynamics of fluorescent particles in homogenous solution or in a living cell with single molecule sensitivity (39, 40). FCS shows fluorescent intensity of fluorescent molecules or particles passing through a detection volume, in which a soluble oligomer is recognized as a single particle with strong intensity. Neuro-2a cells were transfected with siRNA and then with expression vectors for GFP, HttQ23-GFP and HttQ78-GFP and differentiated with db-cAMP. Cell lysates prepared from Htt-GFP-expressing cells were then centrifuged to remove insoluble polyQ aggregates such as visible aggregates under a fluorescent microscope.

First, it was found that there are no differences in fluorescence fluctuation and autocorrelation curves obtained from extracts of both undifferentiated and differentiated cells expressing GFP and HttQ23-GFP and that knockdown of PFD2 and PFD5 did not affect waveforms and autocorrelation curves compared to those for cells without knockdown (Figs. 5A and 5B). Relatively fine waveforms of fluctuations observed in FCS indicate monomers or dimers of HttQ23-GFP. Waveforms from HttQ78-GFP-expressing cells were, on the other hand, found to contain spikes with high fluorescence intensities, and these spikes more frequently appeared when expression of PFD2 and PFD5 was knocked down both in undifferentiated and differentiated cells (Fig. 5A). Autocorrelation curves obtained from undifferentiated and differentiated Htt-Q78-expressing cells were also shifted to the right after expression of PFD2 and PFD5 had been knocked down (Fig. 5B). These results indicate that HttQ78 formed oligomers and that the size of HttQ78-containing soluble species was increased by PFD knockdown.

To estimate the size and proportion of soluble polyQ/Htt species, autocorrelation curves were analyzed by curve fitting using two-component fitting analysis due to the presence of various sizes of soluble Htt aggregates in cell lysates (Table 1). Fast fractions and slow fractions were defined as fraction 1 and fraction 2, respectively. First, it was found both in undifferentiated and differentiated cells that since diffusion time of fraction 1 of HttQ78-GFP (76 μs) was similar to that of GFP (75-79 μs), fraction 1 contained HttQ78-GFP monomers and that diffusion time (106 μs) of fraction 1 of HttQ23-GFP was slightly longer than that of GFP, suggesting that a major fraction of HttQ23-GFP forms dimers under the conditions used. Furthermore, diffusion time of fraction 2 of HttQ23-GFP (660-772 μs) and HttQ78-GFP (542-851 μs) in undifferentiated and differentiated cells was much longer than that of fraction 1, and the average volume of aggregates in fraction 2 was estimated to be 6.1-11.2-fold larger than that in fraction 1, indicating the existence of Htt-soluble aggregates in fraction 2 from both types of cells.

Second, when expression of PFD2 and PFD5 was knocked down by corresponding siRNAs, the diffusion times of fraction 2 in HttQ78-GFP-expressing undifferentiated cells were significantly increased from 558 to 737 and 728 μs, respectively, but contents of fraction 2 (40.9-42.5%) were not affected, indicating that the volume of soluble aggregates were increased by 1.30-1.32 fold and by 2.2-2.3 fold, respectively. After Neuro-2a cells had been differentiated, knockdown of PFD2 and PFD5 expression increased the diffusion times of fraction 2 of HttQ78-GFP from 542 to 756 and 851 μs (1.39-1.58 fold and 2.7-3.9 fold increases in volume, respectively), and these values were larger than those obtained in undifferentiated cells. Diffusion time of fraction 2 of HttQ23-GFP aggregation was, on the other hand,

not affected by prefoldin knockdown. These results revealed that prefoldin knockdown significantly increases the size of soluble aggregates of a pathogenic form of Htt without affecting the number of soluble aggregates, especially in differentiated Neuro-2a cells.

Prefoldin prevents Htt aggregation at the small oligomer stage in vitro.

To investigate more precisely how prefoldin inhibits aggregation of pathogenic Htt, we used an *in vitro* aggregation assay system. First, GST-tagged prefoldin subunits were expressed in and purified from *E. coli*, GST was cleaved off by PreScission protease and the prefoldin complex was reconstituted as described previously (33). GST-HttQ53 and GST-HttQ23 were expressed in and purified from *E. coli*, and addition of PreScission protease into a solution containing GST-HttQ53 or GST-HttQ23 triggered aggregation of HttQ53 and HttQ23. The effect of reconstituted prefoldin on aggregation of HttQ53 and HttQ23 was then examined using filter trap assays. As shown in Fig. 6A, reconstituted prefoldin, but not bovine serum albumin (BSA) as a negative control, strongly inhibited aggregation of HttQ53 in a dose-dependent manner, and complete inhibition of aggregation by prefoldin was observed with a molar ratio of prefoldin to HttQ53 of 1:1. Furthermore, electron microscopic observation revealed the number of large aggregates of HttQ53, but not that of HttQ23, was reduced by prefoldin (Fig. 6B). To quantitatively analyze the aggregation status at the single molecule level, Htt proteins were labeled with Alexa Fluor 488 and analyzed by using total internal reflection fluorescence microscopy (TIRFM) *in vitro* (Figs. 6C-6E and Fig. 7). The results of TIRFM observation at low and high gain levels of an image intensifier showed that aggregation of fluorescently labeled HttQ53 was clearly inhibited by prefoldin and that there was a significantly large number of brighter particles compared to monomers (Figs. 6C and 6D, respectively). After calculation of the size of HttQ53 oligomers, HttQ53 oligomers were found to be mostly dimers and trimers with a small amount of tetramers (Fig. 6E). These results clearly indicate that prefoldin inhibits elongation of aggregates with larger size than that of tetramers, thereby inhibiting further fibrillization of pathogenic Htt.

To examine whether prefoldin also inhibits formation of large oligomers of pathogenic Htt in neuronal cells, Neuro-2a cells were transfected with PFD2 siRNA and PFD5 siRNA and then transfected with a pathogenic form of HttQ78-GFP and differentiated by addition of 5 mM db-cAMP as described above. At 48 h after transfection of siRNAs, proteins extracted from Neuro-2a cells were separated on 5-50% glycerol density gradients. As shown in Fig. 6F, knockdown of PFD2 and PFD5 increased dimer, trimer, tetramer and larger oligomers of HttQ78-GFP, suggesting that prefoldin inhibits large oligomer formation of pathogenic Htt.

Prefoldin prevents specifically Htt aggregation.

We showed that prefoldin knockdown enhances soluble oligomer formation of pathogenic Htt and decreases cell viability. Since knockdown of prefoldin and/or pathogenic Htt give harmful conditions into cells, it is also possible that harmful conditions activate apoptosis pathways independently of prefoldin or pathogenic Htt, resulting in cell death. To examine this, Neuro-2a cells were transfected with PFD2 siRNA and PFD5 siRNA. At 24 h after transfection, cells were treated with two apoptosis inducers, staurosporine and thapsigargin, for 24 h and cell viability was measured by an MTT assay. Staurosporine and thapsigargin are inhibitors of protein kinase C and endoplasmic reticulum Ca^{2+} ATPase, respectively. As shown in Fig. 8A, treatment of staurosporine and thapsigargin reduced cell viability in a dose-dependent manner, but knockdown of PFD2 and PFD5 did not significantly affect staurosporine and thapsigargin-induced cell viability. These results indicate that loss of prefoldin activity targeting pathogenic Htt decreased cell viability. It is also possible that harmful conditions activate autophagy pathways independently of prefoldin or pathogenic Htt, resulting in protein aggregation. To examine this, Neuro-2a cells were transfected with PFD2 siRNA, PFD5 siRNA or non-specific siRNA as a control for 24 h. Cells were then transfected with expression vectors for HttQ78-GFP and Q23-GFP. Twenty –four h after transfection, cells were treated with bafilomycin A1, an inhibitor of the late phase of autophagy, for 12 h. SDS-insoluble aggregates were then examined by a filter trap assay. The results showed that the levels of SDS-insoluble aggregates were increased both in control and bafilomycin A1-treated cells, suggesting that prefoldin inhibits aggregation formation of HttQ78 independently of autophagy induction (Fig. 8B).

DISCUSSION

Since accumulating evidences suggest that formation of pathogenic Htt inclusions is not correlated with neuronal cell death (8, 9), it is thought that soluble oligomers, rather than inclusions, have an important role in neuronal cell toxicity. Oligomerized number and characteristics of pathogenic proteins, however, have not been investigated in detail. The present study first showed that knockdown of PFD2 and PFD5 disrupted prefoldin formation in healthy and pathogenic forms of polyQ or Htt-expressing cells, resulting in accumulation of aggregates of a pathogenic form of polyQ or Htt and in induction of cell death (Figs. 1 and 2). Overexpression of the prefoldin complex reduced accumulation of aggregates of the pathogenic form of Htt (Fig. 3). Knockdown of PFD2 and PFD5 also increased the size of soluble oligomers of the pathogenic form of Htt in cells (Fig. 5). These phenomena observed in polyQ or Htt-expressing cells were also observed in an *in vitro* system comprised of reconstituted prefoldin against purified Htt (Figs. 6A and 6B). Furthermore, *in vitro* single molecule observation by TIRFM analysis demonstrated that prefoldin suppressed Htt aggregation at small

oligomer (dimer to tetramer) stage (Fig. 6E). When PFD2 and PFD5 were knocked down, amounts of dimer, trimer and larger oligomers of pathogenic Htt were increased (Fig. 6F). Furthermore, prefoldin suppresses neuronal cell death, and dead cells did not contain Htt inclusions (Fig. 4C). These results indicate that prefoldin inhibits elongation of large oligomers of the pathogenic Htt, thereby inhibiting subsequent aggregate and inclusion formation, and suggest that soluble large oligomers of polyQ-expanded Htt are more toxic than are inclusions to cells.

Immunofluorescence experiments in this study showed that prefoldin was localized in the cytosol without co-localization with inclusions in Htt-expressing cells, in contrast to the fact that HSP70 was co-localized with inclusions (Fig. 4E). These results suggest that once an inclusion is formed, prefoldin is not able to disrupt inclusion formation and that the inclusion itself is not toxic to cells. Since the localization of prefoldin is reminiscent of that of CCT (21), it is possible that prefoldin cooperates with CCT to prevent the toxicity of Htt at the soluble stage of aggregation or oligomer formation. Since prefoldin interacts with substrate proteins via the tips of tentacles using its hydrophobic surfaces (25, 26, 41), prefoldin may trap misfolded proteins more easily than CCT, which has the substrate recognition site in the cavity near the entrance (42-44).

How does prefoldin inhibit polyglutamine toxicity? Simply thinking from the experimental results in this study, prefoldin delays formation of dimers and trimers of pathogenic Htt oligomers by inhibiting further their elongation, suggesting that pathogenic Htt oligomers of more than tetramers are toxic and that dimers and trimers of pathogenic Htt oligomers are not toxic to cells. On the other hand, considering that prefoldin is a chaperone, following is also possible: Prefoldin may trap misfolded small species (monomers or dimers) and change them into non-toxic small oligomers such as dimers, trimers and tetramers (Fig. 9). Toxic soluble oligomers are thought to exert their toxicity by interacting with other proteins (e.g., coaggregation with functional cellular proteins such as transcription factors TBP and CBP) (38). Co-existence of non-toxic and toxic oligomers of amyloidogenic proteins in cells has indeed been reported (see a review, (45)). If toxic species trapped by prefoldin (e.g., hydrophobic β-sheets) cannot easily be changed into non-toxic forms, prefoldin probably transfers them to CCT or other appropriate chaperones. Prefoldin might also deliver misfolded toxic species to the proteasome for degradation through direct interaction (38, 46).

Knockdown of prefoldin expression increased aggregation of both GFP-Q72 and HttQ78-GFP, the latter of which possesses regions of polyQ and of proteins other than polyQ, indicating that prefoldin recognizes the polyQ sequence rather than a sequence unique to Htt protein. Expression of PFD subunits, particularly PFD2, PFD3 and PFD5, was significantly stimulated after differentiation of Neuro-2a cells (Fig. 2). While knockdown of PFD5 and PFD2 significantly stimulated aggregation and toxicity of pathogenic

Htt in differentiated Neuro-2a cells, knockdown of PFD2, but not that of PFD5, enhanced aggregation and toxicity in undifferentiated Neuro-2a cells. These observations suggest that activity of PFD, including aggregation prevention activity, appears more strongly in neuronal cells than in non-neuronal cells. Intriguingly, PFD1-knockout mice show neuronal loss in the cerebellum and defects in lymphocyte development (47). PFD5-L110R mutant mice also showed that PFD5 missense mutation causes neurodegeneration, photoreceptor degeneration and male infertility (48). These observations suggest that prefoldin plays a pivotal role in maintenance of neuronal cell activity. It has been reported that each of the PFD subunits has its own function, including transcriptional regulation for PFD5 (49, 50) and PFD4 (51) and DNA-binding activity for PFD1 and PFD2 (52), and that there are some distinctive phenotypes between PFD1-null and PFD5-L110R mice (47, 48). PFD5/MM-1 is known to act as a c-Myc-binding protein that suppresses cell growth and transformation independently of the prefoldin complex (49, 53). Furthermore, Tang *et al*. have reported that the expression level of PFD5 mRNA was upregulated in HttQ300-expressing mice (R6/2) despite the fact that mRNA levels of other subunits were unaffected (54). Thus, it is possible that PFD5 alone, or other subunits also, protects neuronal cells through its specific activity. In addition, Simons *et al*. showed that the prefoldin complex interacts with actin and tubulin in a subunit-specific manner: each subunit differentially binds to a target protein (33). CCT also suppresses toxic Htt oligomer formation through specific recognition by its α subunit (55). These observations suggest that particular subunits require their own function to explore their maximal activity in addition to activity as the complex such as prefoldin and CCT.

Knockdown of prefoldin stimulated formation of Htt aggregation and reduced viability of pathogenic Htt-expressing Neuro-2a cells. Since treatment of cells with two apoptosis inducers did not change viability of prefoldin-knockdown cells, (Fig. 7), it is thought that reduced prefoldin activity is directly associated with pathogenic Htt-induced cell toxicity. It has recently been reported that prothymosin-α interacted with pathogenic Htt and suppressed its toxicity through inhibiting pathogenic Htt-induced apoptosis pathway (56). Prothymosin-α was colocalized with Htt in the nucleus and facilitated aggregate formation of pathogenic Htt (56). Although both prefoldin and prothymosin-α show protective activity against toxicity of pathogenic Htt, their mechanisms may be different.

In conclusion, the present study clearly indicates that prefoldin prevents toxicity of polyQ-expanded Htt by inhibiting formation of toxic oligomers. Upregulation of prefoldin by introduction of its subunit genes and by drugs may be useful as a therapy for Huntington disease and other neurodegenerative disorders.

References

1. Walker, F.O. (2007) Huntington's disease. *Lancet*, **369**, 218-228

2. Langbehn, D.R., Brinkman, R.R., Falush, D., Paulsen, J.S., and Hayden, M.R. (2004) A new model for prediction of the age of onset and penetrance for Huntington's disease based on CAG length. *Clin. Genet.* **65**, 267-277

3. Zoghbi, H.Y., and Orr, H.T. (2000) Glutamine repeats and neurodegeneration. *Annu. Rev. Neurosci.* **23**, 217-247
4. Davies, S.W., Turmaine, M., Cozens, B.A., DiFiglia, M., Sharp, A.H., Ross, C.A., Scherzinger, E., Wanker, E.E., Mangiarini, L., and Bates, G.P. (1997) Formation of neuronal intranuclear inclusions underlies the neurological dysfunction in mice transgenic for the HD mutation. *Cell*, **90**, 537-548
5. DiFiglia M, Sapp E, Chase KO, Davies SW, Bates GP, Vonsattel JP, Aronin N. (1997) Aggregation of huntingtin in neuronal intranuclear inclusions and dystrophic neurites in brain. *Science*, **277**, 1990-1993
6. Perutz, M.F., Johnson, T., Suzuki, M., and Finch, J.T. (1994) Glutamine repeats as polar zippers: their possible role in inherited neurodegenerative diseases. *Proc. Natl. Acad. Sci. U.S.A.* **91**, 5355-5358
7. Perutz, M.F., Finch, J.T., Berriman, J., and Lesk, A. (2002) Amyloid fibers are water-filled nanotubes. *Proc. Natl. Acad. Sci. U.S.A.* **99**, 5591-5595
8. Arrasate, M., Mitra, S., Schweitzer, E.S., Segal, M.R., and Finkbeiner, S. (2004) Inclusion body formation reduces levels of mutant huntingtin and the risk of neuronal death. *Nature*, **431**, 805-810
9. Saudou, F., Finkbeiner, S., Devys, D., and Greenberg, M.E. (1998) Huntingtin acts in the nucleus to induce apoptosis but death does not correlate with the formation of intranuclear inclusions. *Cell*, **95**, 55-66
10. Krobitsch, S., and Lindquist, S. (2000) Aggregation of huntingtin in yeast varies with the length of the polyglutamine expansion and the expression of chaperone proteins. *Proc. Natl. Acad. Sci. U.S.A.* **97**, 1589-1594
11. Satyal, S.H., Schmidt, E., Kitagawa, K., Sondheimer, N., Lindquist, S., Kramer, J.M., and Morimoto, R.I. (2000) Polyglutamine aggregates alter protein folding homeostasis in Caenorhabditis elegans. *Proc. Natl. Acad. Sci. U.S.A.* **97**, 5750-5755
12. Wyttenbach, A., Sauvageot, O., Carmichael, J., Diaz-Latoud, C., Arrigo, A.P., and Rubinsztein, D.C. (2002) Heat shock protein 27 prevents cellular polyglutamine toxicity and suppresses the increase of reactive oxygen species caused by huntingtin. *Hum. Mol. Genet.* **11**, 1137-1151

13. Morimoto, R.I. (2008) Proteotoxic stress and inducible chaperone networks in neurodegenerative disease and aging. *Genes Dev.* **22**, 1427-1438

14. Broadley, S.A., and Hartl, F.U. (2009) The role of molecular chaperones in human misfolding diseases. *FEBS Lett.* **583**, 2647-2653

15. Muchowski, P.J., Schaffar, G., Sittler, A., Wanker, E.E., Hayer-Hartl, M.K., and Hartl, F.U. (2000) Hsp70 and hsp40 chaperones can inhibit self-assembly of polyglutamine proteins into amyloid-like fibrils. *Proc. Natl. Acad. Sci. U.S.A.* **97**, 7841-7846

16. Wacker, J.L., Zareie, M.H., Fong, H., Sarikaya, M., and Muchowski, P.J. (2004) Hsp70 and Hsp40 attenuate formation of spherical and annular polyglutamine oligomers by partitioning monomer. *Nat. Struct. Mol. Biol.* **11**, 1215-1222

17. Cummings, C.J., Sun, Y., Opal, P., Antalffy, B., Mestril, R., Orr, H.T., Dillmann, W.H., and Zoghbi, H.Y. (2001) Over-expression of inducible HSP70 chaperone suppresses neuropathology and improves motor function in SCA1 mice. *Hum. Mol. Genet.* **10**, 1511-1518

18. Kazemi-Esfarjani, P., and Benzer, S. (2000) Genetic suppression of polyglutamine toxicity in Drosophila. *Science*, **287**, 1837-1840

19. Warrick, J.M., Chan, H.Y., Gray-Board, G.L., Chai, Y., Paulson, H.L., and Bonini, N.M. (1999) Suppression of polyglutamine-mediated neurodegeneration in Drosophila by the molecular chaperone HSP70. *Nat. Genet.* **23**, 425-428

20. Behrends, C., Langer, C.A., Boteva, R., Bottcher, U.M., Stemp, M.J., Schaffar, G., Rao, B.V., Giese, A., Kretzschmar, H., Siegers, K., and Hartl FU. (2006) Chaperonin TRiC promotes the assembly of polyQ expansion proteins into nontoxic oligomers. *Mol. Cell* **23**, 887-897

21. Kitamura, A., Kubota, H., Pack, C.G., Matsumoto, G., Hirayama, S., Takahashi, Y., Kimura, H., Kinjo, M., Morimoto, R.I., and Nagata, K. (2006) Cytosolic chaperonin prevents polyglutamine toxicity with altering the aggregation state. *Nat. Cell Biol.* **8**, 1163-1170

22. Tam, S., Geller, R., Spiess, C., and Frydman, J. (2006) The chaperonin TRiC controls polyglutamine aggregation and toxicity through subunit-specific interactions. *Nat. Cell Biol.* **8**, 1155-1162

23. Siegers, K., Waldmann, T., Leroux, M.R., Grein, K., Shevchenko, A., Schiebel, E., and Hartl, F.U. (1999) Compartmentation of protein folding in vivo: sequestration of non-native polypeptide by the chaperonin-GimC system. *EMBO J.* **18**, 75-84

24. Vainberg, I.E., Lewis, S.A., Rommelaere, H., Ampe, C., Vandekerckhove, J., Klein, H.L., and Cowan, N.J. (1998) Prefoldin, a chaperone that delivers unfolded proteins to cytosolic chaperonin. *Cell*, **93**, 863-873

25. Siegert, R., Leroux, M.R., Scheufler, C., Hartl, F.U., and Moarefi, I. (2000) Structure of the molecular chaperone prefoldin: unique interaction of multiple coiled coil tentacles with unfolded proteins. *Cell*,

103, 621-632

26. Martin-Benito, J., Gomez-Reino, J., Stirling, P.C., Lundin, V.F., Gomez-Puertas, P., Boskovic, J., Chacon, P., Fernandez, J.J., Berenguer, J., Leroux, M.R., and Valpuesta JM. (2007) Divergent substrate-binding mechanisms reveal an evolutionary specialization of eukaryotic prefoldin compared to its archaeal counterpart. *Structure*, **15**, 101-110
27. Geissler, S., Siegers, K., and Schiebel, E. (1998) A novel protein complex promoting formation of functional alpha- and gamma-tubulin. *EMBO J.* **17**, 952-966
28. Hartl, F.U., and Hayer-Hartl, M. (2002) Molecular chaperones in the cytosol: from nascent chain to folded protein. *Science*, **295**, 1852-1858
29. Sakono, M., Zako, T., Ueda, H., Yohda, M., and Maeda, M. (2008) Formation of highly toxic soluble amyloid beta oligomers by the molecular chaperone prefoldin. *FEBS J.* **275**, 5982-5993
30. Kouroku, Y., Fujita, E., Tanida, I., Ueno, T., Isoai, A., Kumagai, H., Ogawa, S., Kaufman, R.J., Kominami, E., and Momoi, T. (2007) ER stress (PERK/eIF2alpha phosphorylation) mediates the polyglutamine-induced LC3 conversion, an essential step for autophagy formation. *Cell Death Differ.* **14**, 230-239
31. Schaffar, G., Breuer, P., Boteva, R., Behrends, C., Tzvetkov, N., Strippel, N., Sakahira, H., Siegers, K., Hayer-Hartl, M., and Hartl, F.U. (2004) Cellular toxicity of polyglutamine expansion proteins: mechanism of transcription factor deactivation. *Mol. Cell* **15**, 95-105
32. Wanker, E.E., Scherzinger, E., Heiser, V., Sittler, A., Eickhoff, H., and Lehrach, H. (1999) Membrane filter assay for detection of amyloid-like polyglutamine-containing protein aggregates. *Methods Enzymol.* **309**, 375-386
33. Simons, C.T., Staes, A., Rommelaere, H., Ampe, C., Lewis, S.A., and Cowan, N.J. (2004) Selective contribution of eukaryotic prefoldin subunits to actin and tubulin binding. *J. Biol. Chem.* **279**, 4196-4203
34. Taguchi, H., Ueno, T., Tadakuma, H., Yoshida, M., and Funatsu, T. (2001) Single-molecule observation of protein-protein interactions in the chaperonin system. *Nat. Biotechnol.* **19**, 861-865
35. Zako, T., Iizuka, R., Okochi, M., Nomura, T., Ueno, T., Tadakuma, H., Yohda, M., and Funatsu, T. (2005) Facilitated release of substrate protein from prefoldin by chaperonin. *FEBS Lett.* **579**, 3718-3724
36. Gell, C., Brockwell, D., and Smith, A. (2006) *Handbook of Single Molecule Fluorescence Spectroscopy*. Oxford University Press, New York.
37. Leake, M.C., Chandler, J.H., Wadhams, G.H., Bai, F., Berry, R.M., and Armitage, J.P. (2006) Stoichiometry and turnover in single, functioning membrane protein complexes. *Nature*, **443**, 355-358

38. Miyazawa, M., Tashiro, E., Kitaura, H., Maita, H., Suto, H., Iguchi-Ariga, S.M., and Ariga, H. (2011) Prefoldin subunits are protected from ubiquitin-proteasome system-mediated degradation by forming complex with other constituent subunits. *J. Biol. Chem*, **286**, 19191-19203

39. Eigen, M., and Rigler, R. (1994) Sorting single molecules: application to diagnostics and evolutionary biotechnology. *Proc. Natl. Acad. Sci. U.S.A.* **91**, 5740-5747

40. Elson, E.L. (2001) Fluorescence correlation spectroscopy measures molecular transport in cells. *Traffic*, **2**, 789-796

41. Martin-Benito, J., Boskovic, J., Gomez-Puertas, P., Carrascosa, J.L., Simons, C.T., Lewis, S.A., Bartolini, F., Cowan, N.J., and Valpuesta, J.M. (2002) Structure of eukaryotic prefoldin and of its complexes with unfolded actin and the cytosolic chaperonin CCT. *EMBO J.* **21**, 6377-6386

42. Ditzel, L., Lowe, J., Stock, D., Stetter, K.O., Huber, H., Huber, R., and Steinbacher, S. (1998) Crystal structure of the thermosome, the archaeal chaperonin and homolog of CCT. *Cell*, **93**, 125-138

43. Klumpp, M., Baumeister, W., and Essen, L.O. (1997) Structure of the substrate binding domain of the thermosome, an archaeal group II chaperonin. *Cell*, **91**, 263-270

44. Llorca, O., Smyth, M.G., Carrascosa, J.L., Willison, K.R., Radermacher, M., Steinbacher, S., and Valpuesta, J.M. (1999) 3D reconstruction of the ATP-bound form of CCT reveals the asymmetric folding conformation of a type II chaperonin. *Nat. Struct. Biol.* **6**, 639-642

45. Uversky, V.N. (2010) Mysterious oligomerization of the amyloidogenic proteins. *FEBSJ* .**277**, 2940-2953

46. Mousnier, A., Kubat, N., Massias-Simon, A., Segeral, E., Rain, J.C., Benarous, R., Emiliani, S., and Dargemont, C. (2007) von Hippel Lindau binding protein 1-mediated degradation of integrase affects HIV-1 gene expression at a postintegration step. *Proc. Natl. Acad. Sci. U.S.A.* **104**, 13615-13620

47. Cao, S., Carlesso, G., Osipovich, A., Llanes, J., Lin, Q., Hoek, K., Khan, W., and Ruley, H. (2008) Subunit 1 of the prefoldin chaperone complex is required for lymphocyte development and function. *J. Immunol.* **181**, 476-560

48. Lee, Y., Smith, R.S., Jordan, W., King, B.L., Won, J., Valpuesta, J.M., Naggert, J.K., and Nishina, P.M. (2011) Prefoldin 5 is required for normal sensory and neuronal development in a murine model. *J. Biol. Chem.* **286**, 726-736

49. Mori, K., Maeda, Y., Kitaura, H., Taira, T., Iguchi-Ariga, S.M., and Ariga, H. (1998) MM-1, a novel c-Myc-associating protein that represses transcriptional activity of c-Myc. *J. Biol. Chem.* **273**, 29794-29800

50. Satou, A., Taira, T., Iguchi-Ariga, S.M., and Ariga, H. (2001) A novel transrepression pathway of c-Myc. Recruitment of a transcriptional corepressor complex to c-Myc by MM-1, a c-Myc-binding protein. *J. Biol. Chem.* **276**, 46562-46567

51. Iijima, M., Kano, Y., Nohno, T., and Namba, M. (1996) Cloning of cDNA with possible transcription factor activity at the G1-S phase transition in human fibroblast cell lines. *Acta Medica Okayama*, **50**, 73-77

52. Myung, J.K., Afjehi-Sadat, L., Felizardo-Cabatic, M., Slavc, I., and Lubec, G. (2004) Expressional patterns of chaperones in ten human tumor cell lines. *Proteome Sci.* **2**, 8

53. Fujioka, Y., Taira, T., Maeda, Y., Tanaka, S., Nishihara, H., Iguchi-Ariga, S.M., Nagashima, K., and Ariga, H. (2001) MM-1, a c-Myc-binding protein, is a candidate for a tumor suppressor in leukemia/lymphoma and tongue cancer. *J. Biol. Chem.* **276**, 45137-45144

54. Tang, B., Seredenina, T., Coppola, G., Kuhn, A., Geschwind, D.H., Luthi-Carter, R., and Thomas, E.A. (2011) Gene expression profiling of R6/2 transgenic mice with different CAG repeat lengths reveals genes associated with disease onset and progression in Huntington's disease. *Neurobiol. Dis.* **42**, 459-467

55. Tam, S., Spiess, C., Auyeung, W., Joachimiak, L., Chen, B., Poirier, M.A., and Frydman, J. (2009) The chaperonin TRiC blocks a huntingtin sequence element that promotes the conformational switch to aggregation. *Nat. Struct. Mol. Biol.* **16**, 1279-1285

56. Dong, G., Callegari, E.A., Gloeckner, C.J., Ueffing, M., and Wang, H. (2012) Prothymosin-α interacts with mutant huntingtin and suppresses its cytotoxicity in cell culture. *J. Biol. Chem.* **287**, 1279-1289

FOOTNOTES

We thank Profs. R. I. Morimoto and F. U. Hartl for providing expression vectors for Htt and for GST-Htt, respectively. This work was supported by grants-in-aid from the Ministry of Education, Culture, Sports, Science and Technology (MEXT) and from New Energy and Industrial Technology Development Organization (NEDO) and by the Program for Promotion of Fundamental Studies in Health Sciences of the National Institute of Biomedical Innovation (NIBIO) in Japan.

FIGURE LEGENDS

Figure 1. RNAi-mediated knockdown of PFD2 significantly stimulates aggregation of polyQ/Htt in undifferentiated neuronal cells.

A. Neuro-2a cells were transfected with PFD2 siRNA, PFD5 siRNA or non-specific siRNA (NS) as a control. Proteins were extracted at 48 h after transfection and analyzed by Western blotting with antibodies against prefoldin subunits.

B. Cell lysates prepared from siRNA-transfected cells as described in the legend for Fig. 1C were fractionated on a 5-15% glycerol density gradient, and proteins in each fraction were analyzed by Western

blotting with anti-PFD2 and anti-PFD5 antibodies.

C. Fluorescent microscopic images of GFP (left), GFP-polyQ (middle) and Htt-GFP (right) expressed in Neuro-2a cells. Neuro-2a cells were transfected with PFD2 siRNA, PFD5 siRNA or non-specific siRNA as a control for 24 h. Cells were then transfected with expression vectors for GFP-Q72, GFP-Q11, HttQ78-GFP, HttQ23-GFP or GFP alone, and cell images were obtained at 48 h after siRNA transfection.

D. Aggregate-containing cells were counted in cell images of Fig. 1C, and data are shown as mean ± S.D. of three experiments. *p<0.05 and ***p<0.001 compared to control (NS).

E and F. Filter-trap assays of SDS-insoluble aggregates of GFP-polyQ (G) and Htt-GFP (H). Cell lysates prepared from siRNA-transfected cells as described in the legend for Fig. 1C were passed through a cellulose acetate membrane and reacted with an anti-GFP antibody.

Figure 2. RNAi-mediated knockdown of PFD2 and PFD5 significantly stimulates aggregation of polyQ/Htt in differentiated neuronal cells.

A. Neuro-2a cells were transfected with PFD2 siRNA, PFD5 siRNA or non-specific siRNA as a control and treated with 5 mM dibutyryl cyclic AMP (db-cAMP) at 4 h after transfection. Proteins were extracted at 48 h after siRNA transfection and analyzed by Western blotting with antibodies against prefoldin subunits.

B. Neuro-2a cells were treated as described in the legend for Fig. 2A. Proteins extracted were analyzed by Western blotting with anti-PFD2, anti-PFD5, anti-HSP70, anti-HSC70, anti-HSP40, anti-CCTα and anti-GAPDH antibodies.

C-E. Neuro-2a cells were transfected with PFD2 siRNA, PFD5 siRNA or non-specific siRNA as a control. At 24 h after transfection, cells were transfected with expression vectors for GFP (C), GFP-polyQ (D) and Htt-GFP (E) and treated with 5 mM db-cAMP at 4 h after transfection. Aggregate-containing cells were counted at 48 h after transfection of GFP, GFP-polyQ and Htt-GFP. n=3.

F and G. Neuro-2a cells were treated as described in the legend for Figs. 2C-2E, and protein extracts prepared from cells were subjected to filter-trap assays as described in Experimental procedures.

Figure 3. Overexpression of prefoldin inhibits aggregation of polyQ/Htt.

Neuro-2a cells were transfected with 5 and 10 ng expression vectors for 6 prefoldin subunits. Twenty-four h after transfection, cells were transfected with an expression vector for Htt23-polyQ-GFP or Htt78-polyQ-GFP and differentiated into neuronal cells by addition of db-cAMP. Forty-eight h after transfection, protein extracts prepared from cells were subjected to filter-trap assays as described in Experimental procedures.

Figure 4. Dead cells did not contain Htt inclusions and prefoldin was not colocalized with inclusions.

A and B. Neuro-2a cells were transfected with PFD2 siRNA, PFD5 siRNA or non-specific siRNA (NS). At 24 h after transfection, cells were transfected with expression vectors for GFP and Htt-GFP and treated with 0 or 5 mM db-cAMP at 4 h after transfection (A and B, respectively). Cells expressing HttQ78-GFP (green) were stained with propidium iodide (red) as an indicator of cell death at 48 h after transfection of GFP and Htt-GFP, and the number of propidium iodide-stained cells in GFP-expressing cells was counted (n=3). More than 92% of cell death occurred without inclusion formation, and knockdown of PFD2 and PFD5 resulted in no significant difference in the proportion. *$p < 0.05$, **$p < 0.01$, ***$p < 0.001$ versus control (NS).

C and D. Dead cells as shown in Figs. 4A and 4B were categorized into two groups by GFP signals, inclusion-containing cells and diffusely distributed cells. The numbers of the categorized cells were counted.

E. Neuro-2a cells were transfected with an expression vector for HttQ78-GFP. At 48 h after transfection, cells were fixed, immunostained with anti-PFD2, anti-PFD5, anti-CCTβ, anti-HSC70 and anti-GFP antibodies, and then reacted with an Alexa Fluor 594-conjugated anti-IgG antibody. Cell images were then obtained under a confocal laser microscope. Inserts show enlarged views of inclusions.

Figure 5. Prefoldin-knockdown increased soluble aggregates of polyQ-expanded Htt.

Neuro-2a cells were transfected with PFD2 siRNA, PFD5 siRNA or non-specific siRNA as a control. At 24 h after transfection, cells were transfected with expression vectors for HttQ78-GFP, HttQ23-GFP and GFP and treated with 5 mM db-cAMP at 4 h after transfection. At 48 h after transfection of HttQ78-GFP, HttQ23-GFP and GFP, cell lysates prepared from cells were centrifuged at 17,400 x g and supernatants were analyzed by FCS.

A. Count rates of fluorescence fluctuation for 30 s are shown as blue, pink and gray lines from PFD2 siRNA-, PFD5 siRNA- and non-specific siRNA-transfected cells, respectively. Arrows indicate signals of strong fluorescence intensity from soluble GFP-Htt aggregates.

B. Normalized autocorrelation curves of Htt-GFP proteins in FCS are shown.

Figure 6. Prefoldin directly suppresses aggregation of polyQ-expanded Htt.

A. Filter trap assays of HttQ53 and HttQ23 aggregation in the presence and absence of prefoldin. Aggregation of HttQ53 and HttQ23 was initiated by addition of PreScission protease to a solution containing GST-HttQ53 and GST-HttQ23 and the solution was incubated at 30°C for 12 h. Aggregates were then trapped on filters and analyzed by immunoblotting with an anti-GFP antibody. Bovine serum albumin was used as a control.

B. Electron microscopic analysis of HttQ53 and HttQ23 aggregation in the presence or absence of prefoldin. Bar indicates a size of 1 μm.

C. Fluorescent microscopic observation of Alexa Fluor 488-labeled HttQ53 aggregation in the presence or absence of prefoldin by the TIRFM system. Samples were diluted 10 times immediately before observation under a fluorescent microscope. The gain level of the image intensifier was set at 1.3. Bar indicates a size of 10 μm.

D. Distribution of the number of HttQ53 molecules per particle. Fluorescence intensity of the single dye was determined by distribution of photobleaching unitary step intensities of labeled monomer proteins (Supplementary Figs. S4A and S4B). The number of HttQ53 molecules per particle was determined by dividing fluorescence intensities of particles by that of single dye after adjusting light attenuation levels by ND filters (Supplementary Fig. 4E).

E. Observation of a single molecule of Alexa Fluor 488 labeled-HttQ53 aggregation in the presence of prefoldin by the TIRFM system. Samples were diluted 3000 times immediately before observation under a fluorescent microscope. The gain level of the image intensifier was set at 4.2. Bar indicates a size of 10 μm.

F. Detection of pathogenic Htt oligomers under prefoldin-knockdown conditions. Differentiated Neuro-2a cell lysates containing HttQ78-GFP were prepared as described in Experimental procedures and were fractionated on a 5-50% glycerol density gradient. Proteins in each fraction were analyzed by Western blotting with an anti-GFP antibody.

Figure 7. TIRFM analyses of Htt oligomers.

A. Photobleaching of Alexa Fluor 488-HttQ53 molecule.

B. Distribution of photobleaching unitary step intensity of Alexa Fluor 488 dye (N=209). The peak fluorescence intensity was estimated by Gaussian fitting and shown as mean ± S.D.

C and D. Fluorescence intensities of single particles of Alexa Fluor 488-GST-HttQ53 (c) and Alexa Fluor 488-GST-HttQ23 (D) were measured before (white column) and after (black column) incubation of proteins with PreScission protease in the presence of prefoldin for 13 h. Samples were diluted 3000-fold and illuminated by a blue laser (488 nm, 11.8 mW). The gain level of the image intensifier was set at 4.2. To correctly measure the intensity of Alexa Fluor 488-GST-HttQ53 samples that had been incubated with prefoldin for 13 h, an ND40 filter (5.2 mW) was used to avoid saturation of fluorescence intensities, and their fluorescence intensities were multiplied by 2.4, which was calculated from the linear correlation between laser power and fluorescent intensity shown in panel E.

E. Fluorescent intensities of FluoSpheres (0.1 μm diameter and yellow-green, Molecular Probes) were excited with a blue laser using different ND filters. Each laser beam power was measured by a power

meter. Fluorescence intensity was decreased to 41.5±1.9% (1/2.4-fold) by the ND40 filter compared to that in the absence of an ND filter (ND100).

Figure 8. Prefoldin specifically affects cell viability by targeting polyQ-expanded Htt.

A. Neuro-2a cells in 96-well plats were transfected with PFD2 siRNA, PFD5 siRNA or non-specific siRNA (NS) as a control. At 24 h after transfection, cells were treated with various amounts of staurosporine (A-a) and thapsigargin (A-b) for 24 h, and cell viability was examined by MTT assays. A negative control shown as "nega" is cells that were added with a transfection buffer and DMSO and then killed with 20% Triton-X100 before measuring their viability. A positive control shown as "posi" is cells that were added with a transfection buffer and DMSO.

B. Neuro-2a cells were transfected with PFD2 siRNA, PFD5 siRNA or non-specific siRNA as a control for 24 h. Cells were then transfected with expression vectors for HttQ78-GFP and HttQ23-GFP. Twenty –four h after transfection, cells were treated with bafilomycin A1, an inhibitor of the late phase of autophagy, for 12 h. SDS-insoluble aggregates were then examined by a filter trap assay as described in Experimental procedures.

Figure 9. Schematic model of action of prefoldin against pathogenic forms of Huntingtin.

Table 1. Diffusion time and content of Htt proteins under normal and prefoldin-knockdown conditions

			rapid fraction (F1)		slow fraction (F2)		
db-cAMP	**expression**	**siRNA**	**DT (μs)**	**content (%)**	**DT (μs)**	**content (%)**	**X^2**
0 mM	GFP	NS	78 ± 5	100			$7.79 \pm 4.77 \times 10^{-7}$
0 mM	GFP	PFD2	78 ± 8	100			$9.79 \pm 7.82 \times 10^{-7}$
0 mM	GFP	PFD5	79 ± 7	100			$6.75 \pm 4.70 \times 10^{-7}$
5 mM	GFP	NS	78 ± 9	100			$2.11 \pm 5.47 \times 10^{-7}$
5 mM	GFP	PFD2	78 ± 7	100			$2.19 \pm 1.08 \times 10^{-7}$
5 mM	GFP	PFD5	75 ± 6	100			$4.81 \pm 3.31 \times 10^{-7}$
0 mM	HttQ23-GFP	NS	106	59.7	698 ± 50	40.3 ± 10.5	$2.00 \pm 0.46 \times 10^{-6}$
0 mM	HttQ23-GFP	PFD2	106	57.0	665 ± 38	43.0 ± 14.4	$3.71 \pm 0.68 \times 10^{-6}$
0 mM	HttQ23-GFP	PFD5	106	57.6	772 ± 47	42.4 ± 13.4	$2.89 \pm 1.45 \times 10^{-6}$
0 mM	HttQ78-GFP	NS	76	58.0	558 ± 33	42.0 ± 6.7	$3.68 \pm 4.74 \times 10^{-5}$
0 mM	HttQ78-GFP	PFD2	76	57.5	737 ± 75	42.5 ± 1.5	$2.69 \pm 0.31 \times 10^{-5}$
0 mM	HttQ78-GFP	PFD5	76	59.1	728 ± 127	40.9 ± 6.3	$1.60 \pm 0.88 \times 10^{-5}$
5 mM	HttQ23-GFP	NS	106	55.6	650 ± 69	44.4 ± 2.4	$4.75 \pm 0.29 \times 10^{-7}$
5 mM	HttQ23-GFP	PFD2	106	50.9	713 ± 59	49.1 ± 3.2	$7.20 \pm 0.30 \times 10^{-7}$
5 mM	HttQ23-GFP	PFD5	106	46.9	701 ± 11	53.1 ± 6.8	$0.69 \pm 4.29 \times 10^{-6}$
5 mM	HttQ78-GFP	NS	76	54.5	542 ± 50	45.5 ± 1.7	$0.59 \pm 3.34 \times 10^{-6}$
5 mM	HttQ78-GFP	PFD2	76	52.5	756 ± 140	47.5 ± 3.1	$1.23 \pm 4.92 \times 10^{-6}$
5 mM	HttQ78-GFP	PFD5	76	51.7	851 ± 194	48.3 ± 5.9	$0.28 \pm 2.52 \times 10^{-5}$

Diffusion time (DT) was estimated by curve fitting of the autocorrelation curves of FCS analysis of Htt-GFP at 48 h (mean ± s.d., n=3). The data of GFP were analyzed by a one-component model, whereas the HttQ23 and HttQ78-GFP data were analyzed by a two-component model to provide the best fit. Significance of curve fitting was analyzed by the X^2 test. To accurately estimate the diffusion time and content of the second component (soluble aggregates) at 48 h, the diffusion time of the first component was fixed to the values of monomers that were determined at 24 h.

Figure 1

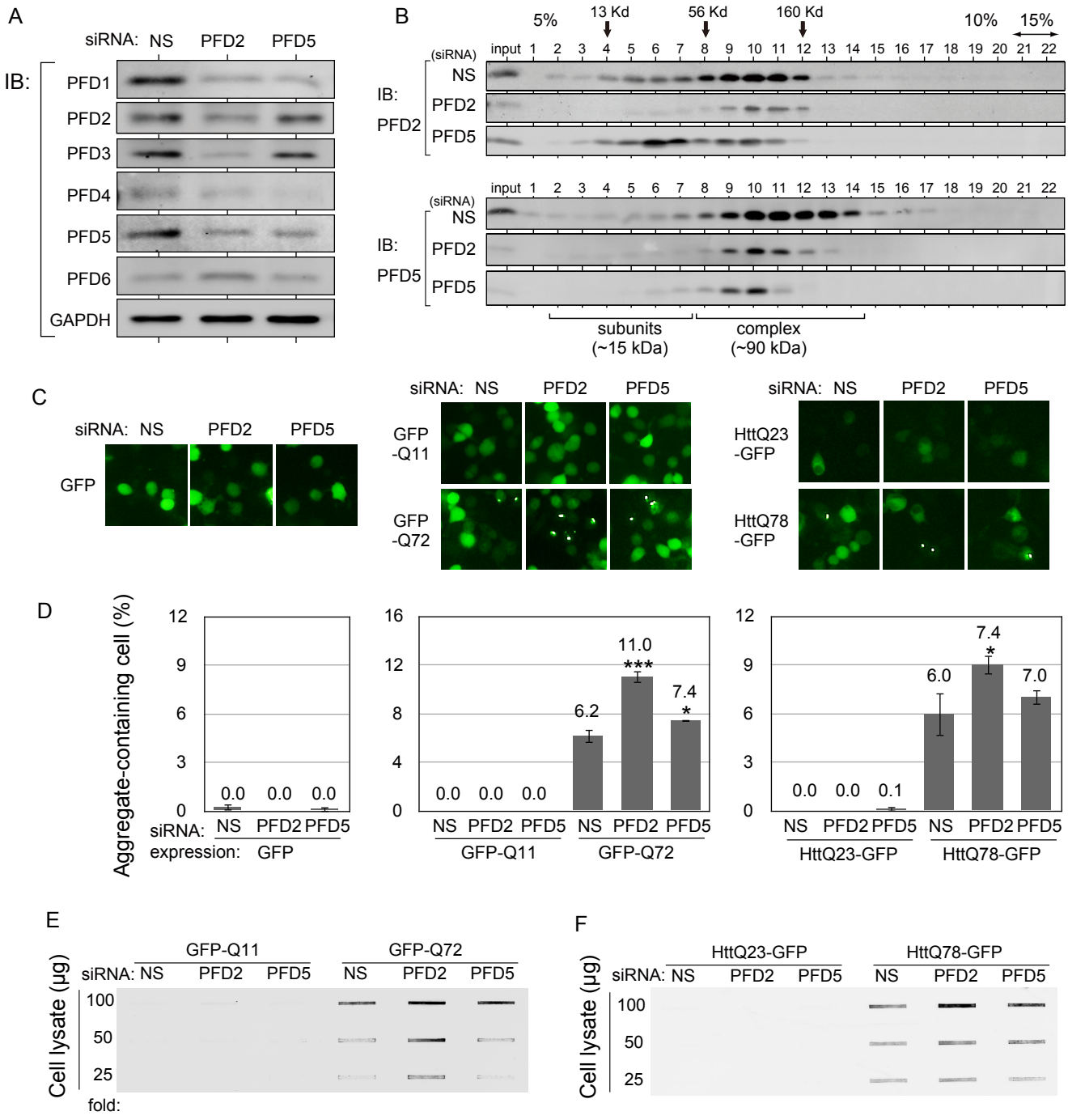
A
siRNA: NS PFD2 PFD5
IB:
PFD1
PFD2
PFD3
PFD4
PFD5
PFD6
GAPDH
B
5%
13 Kd
56 Kd
160 Kd
10%
15%
(siRNA)
input 1 2 3 4 5 6 7 8 9 10 11 12 13 14 15 16 17 18 19 20 21 22
NS
IB:
PFD2
PFD5
subunits (~15 kDa)
complex (~90 kDa)
C
siRNA: NS PFD2 PFD5
GFP
GFP -Q11
GFP -Q72
HttQ23 -GFP
HttQ78 -GFP
D
Aggregate-containing cell (%)
0.0 0.0 0.0
6.2
11.0 ***
7.4 *
0.1
6.0
7.4 *
7.0
siRNA: NS PFD2 PFD5
expression: GFP
GFP-Q11
GFP-Q72
HttQ23-GFP
HttQ78-GFP
E
GFP-Q11
GFP-Q72
siRNA: NS PFD2 PFD5 NS PFD2 PFD5
Cell lysate (μg)
100
50
25
fold:
F
HttQ23-GFP
HttQ78-GFP
siRNA: NS PFD2 PFD5 NS PFD2 PFD5
Cell lysate (μg)
100
50
25

Figure 2

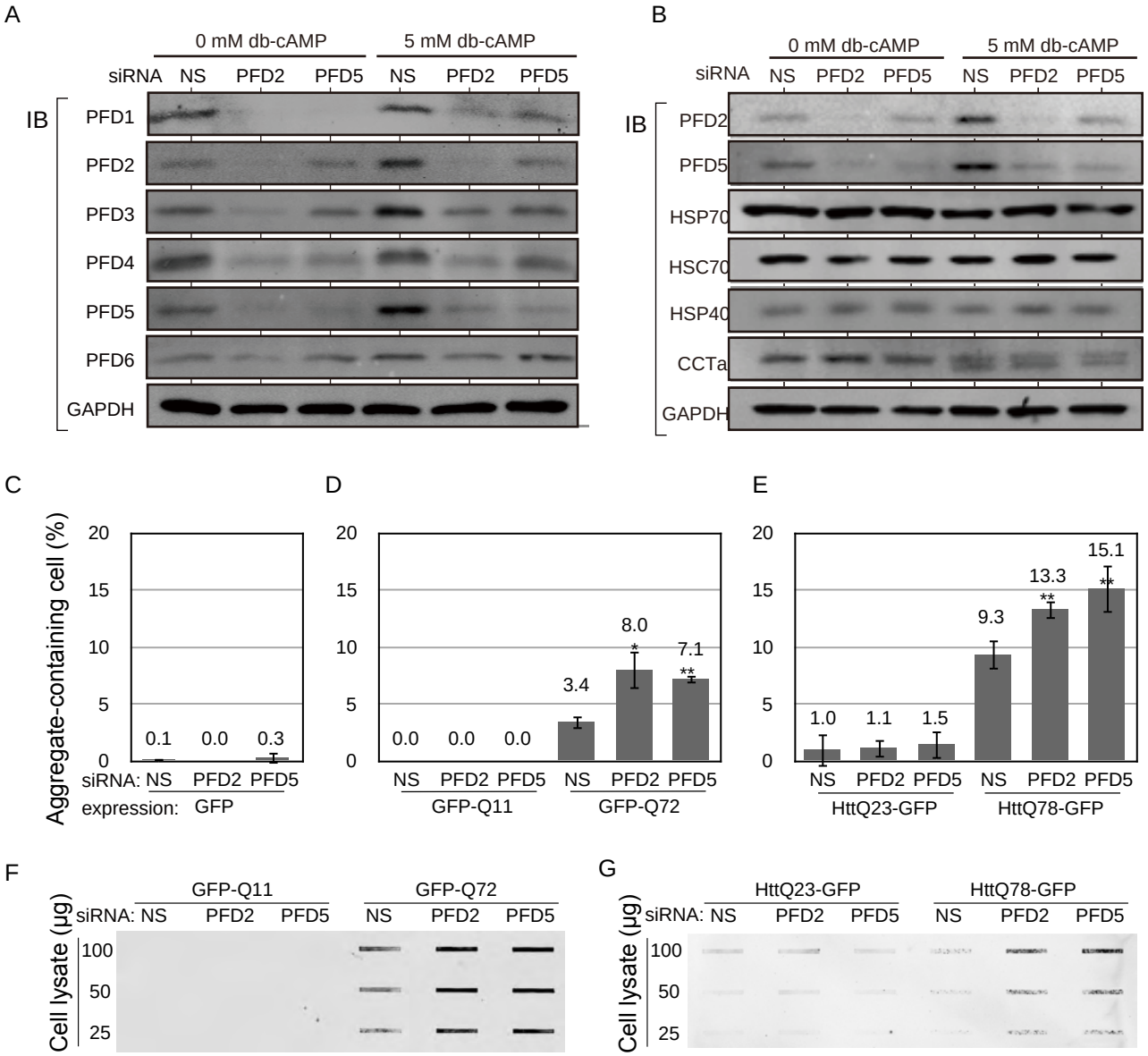
A
0 mM db-cAMP
5 mM db-cAMP
siRNA NS PFD2 PFD5 NS PFD2 PFD5
IB
PFD1
PFD2
PFD3
PFD4
PFD5
PFD6
GAPDH
B
0 mM db-cAMP
5 mM db-cAMP
siRNA NS PFD2 PFD5 NS PFD2 PFD5
IB
PFD2
PFD5
HSP70
HSC70
HSP40
CCTa
GAPDH
C
Aggregate-containing cell (%)
20
15
10
5
0
0.1
0.0
0.3
siRNA: NS PFD2 PFD5
expression: GFP
D
20
15
10
5
0
0.0
0.0
0.0
3.4
8.0
*
7.1
**
NS PFD2 PFD5 NS PFD2 PFD5
GFP-Q11
GFP-Q72
E
20
15
10
5
0
1.0
1.1
1.5
9.3
13.3
**
15.1
**
NS PFD2 PFD5 NS PFD2 PFD5
HttQ23-GFP
HttQ78-GFP
F
GFP-Q11
GFP-Q72
siRNA: NS PFD2 PFD5 NS PFD2 PFD5
Cell lysate (μg)
100
50
25
G
HttQ23-GFP
HttQ78-GFP
siRNA: NS PFD2 PFD5 NS PFD2 PFD5
Cell lysate (μg)
100
50
25

Figure 3

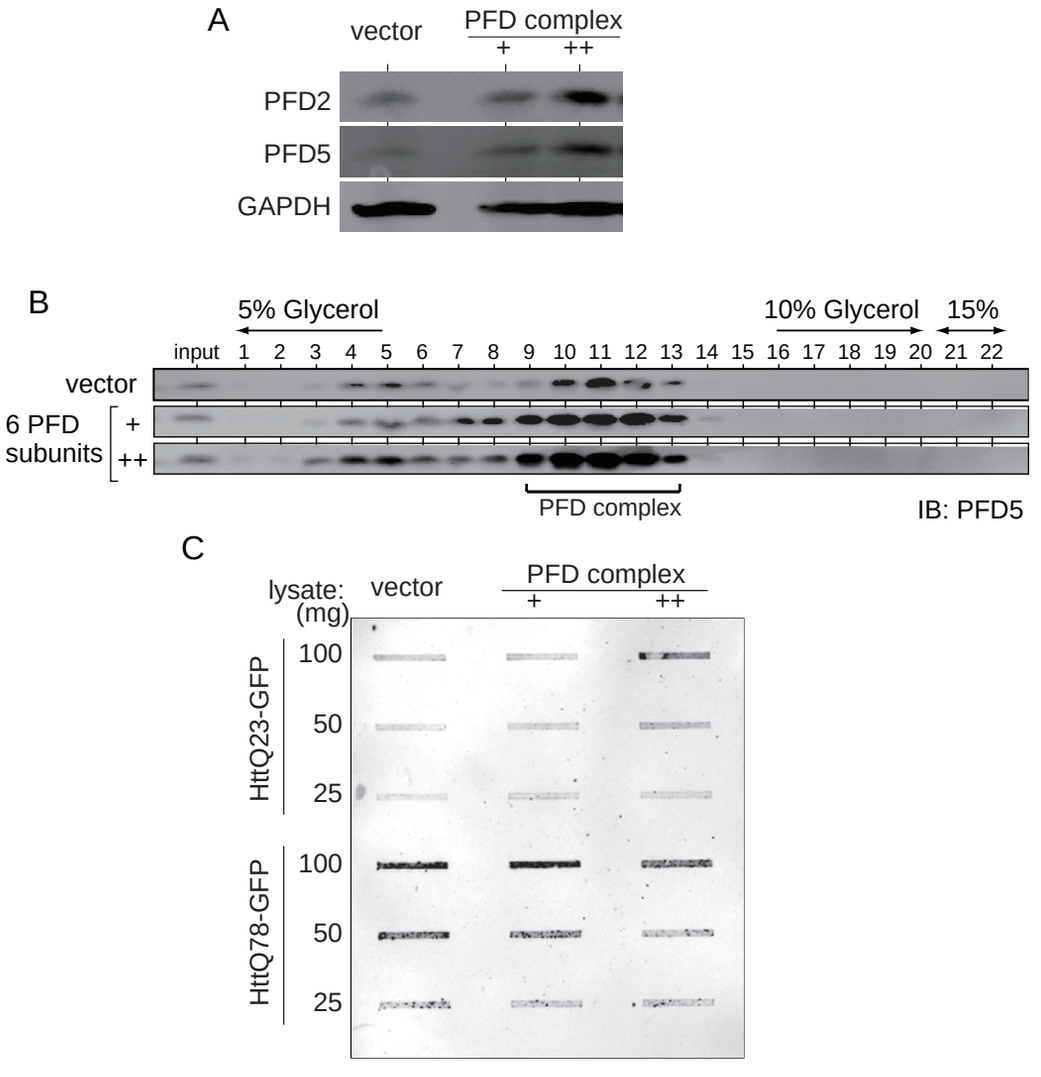
A
vector
PFD complex
+
++
PFD2
PFD5
GAPDH
B
5% Glycerol
10% Glycerol
15%
input 1 2 3 4 5 6 7 8 9 10 11 12 13 14 15 16 17 18 19 20 21 22
vector
6 PFD subunits
+
++
PFD complex
IB: PFD5
C
lysate: (mg)
vector
PFD complex
+
++
HttQ23-GFP
100
50
25
HttQ78-GFP
100
50
25

Figure 4

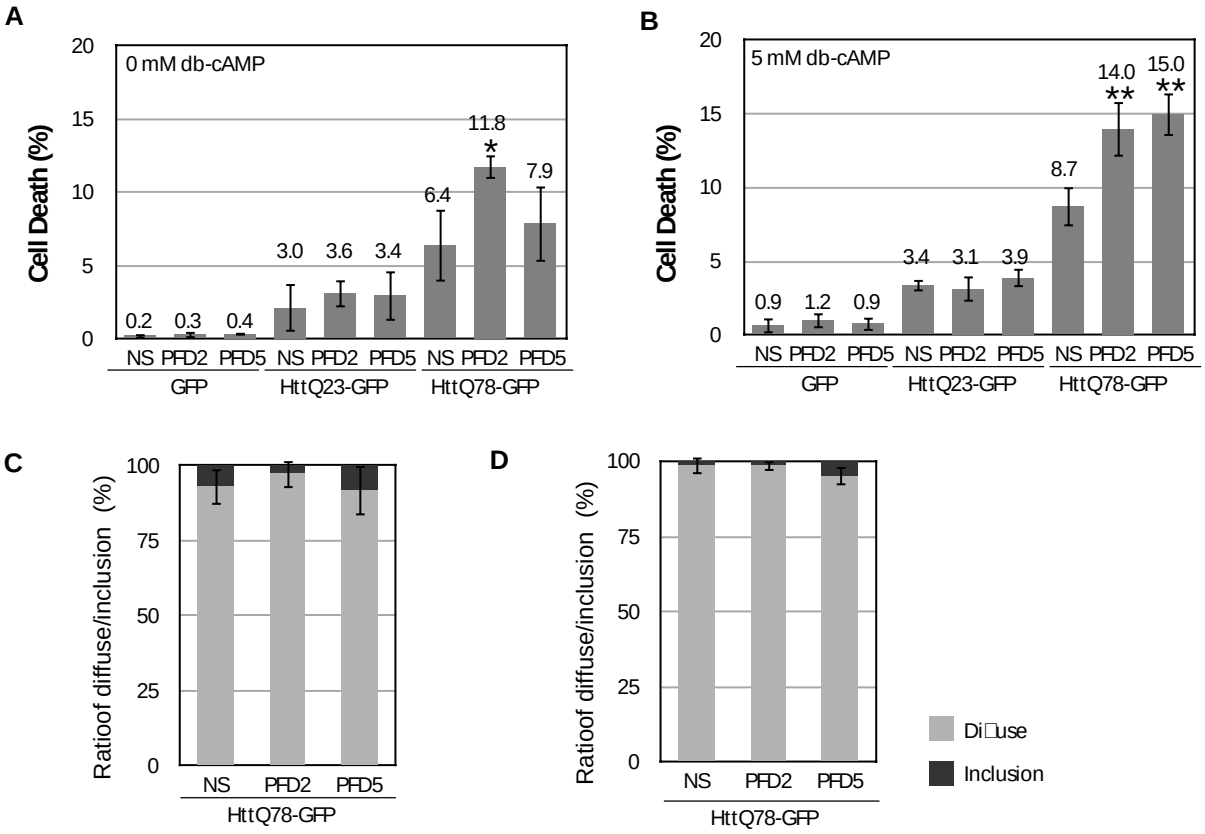
A
0 mM db-cAMP
Cell Death (%)
20
15
10
5
0
0.2
0.3
0.4
3.0
3.6
3.4
6.4
11.8
*
7.9
NS PFD2 PFD5 NS PFD2 PFD5 NS PFD2 PFD5
GFP
HttQ23-GFP
HttQ78-GFP
B
5 mM db-cAMP
Cell Death (%)
0.9
1.2
0.9
3.4
3.1
3.9
8.7
14.0
**
15.0
**
NS PFD2 PFD5 NS PFD2 PFD5 NS PFD2 PFD5
GFP
HttQ23-GFP
HttQ78-GFP
C
Ratioof diffuse/inclusion (%)
100
75
50
25
0
NS PFD2 PFD5
HttQ78-GFP
D
Ratioof diffuse/inclusion (%)
100
75
50
25
0
NS PFD2 PFD5
HttQ78-GFP
Di□use
Inclusion

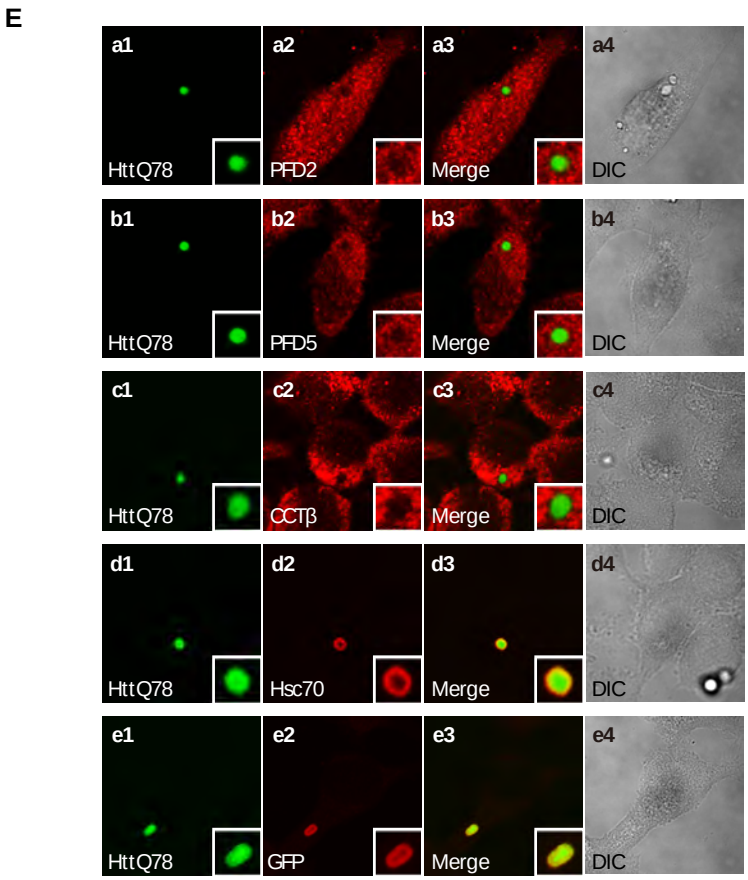
E
a1
HttQ78
a2
PFD2
a3
Merge
a4
DIC
b1
HttQ78
b2
PFD5
b3
Merge
b4
DIC
c1
HttQ78
c2
CCTβ
c3
Merge
c4
DIC
d1
HttQ78
d2
Hsc70
d3
Merge
d4
DIC
e1
HttQ78
e2
GFP
e3
Merge
e4
DIC

Figure 5

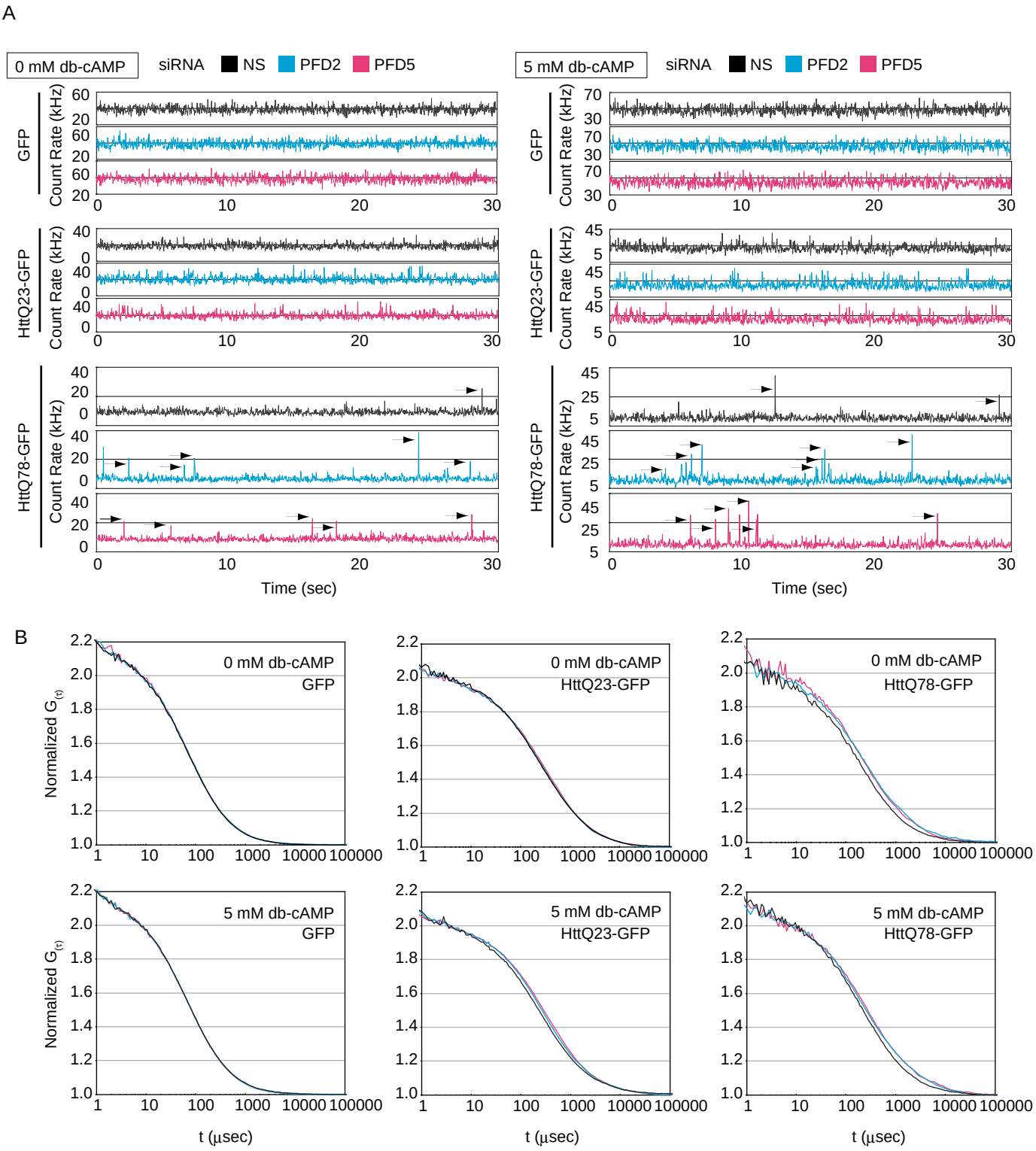
A
0 mM db-cAMP
siRNA
NS
PFD2
PFD5
5 mM db-cAMP
GFP
HttQ23-GFP
HttQ78-GFP
Count Rate (kHz)
Time (sec)
B
Normalized G(τ)
0 mM db-cAMP
GFP
HttQ23-GFP
HttQ78-GFP
5 mM db-cAMP
t (µsec)

Figure 6

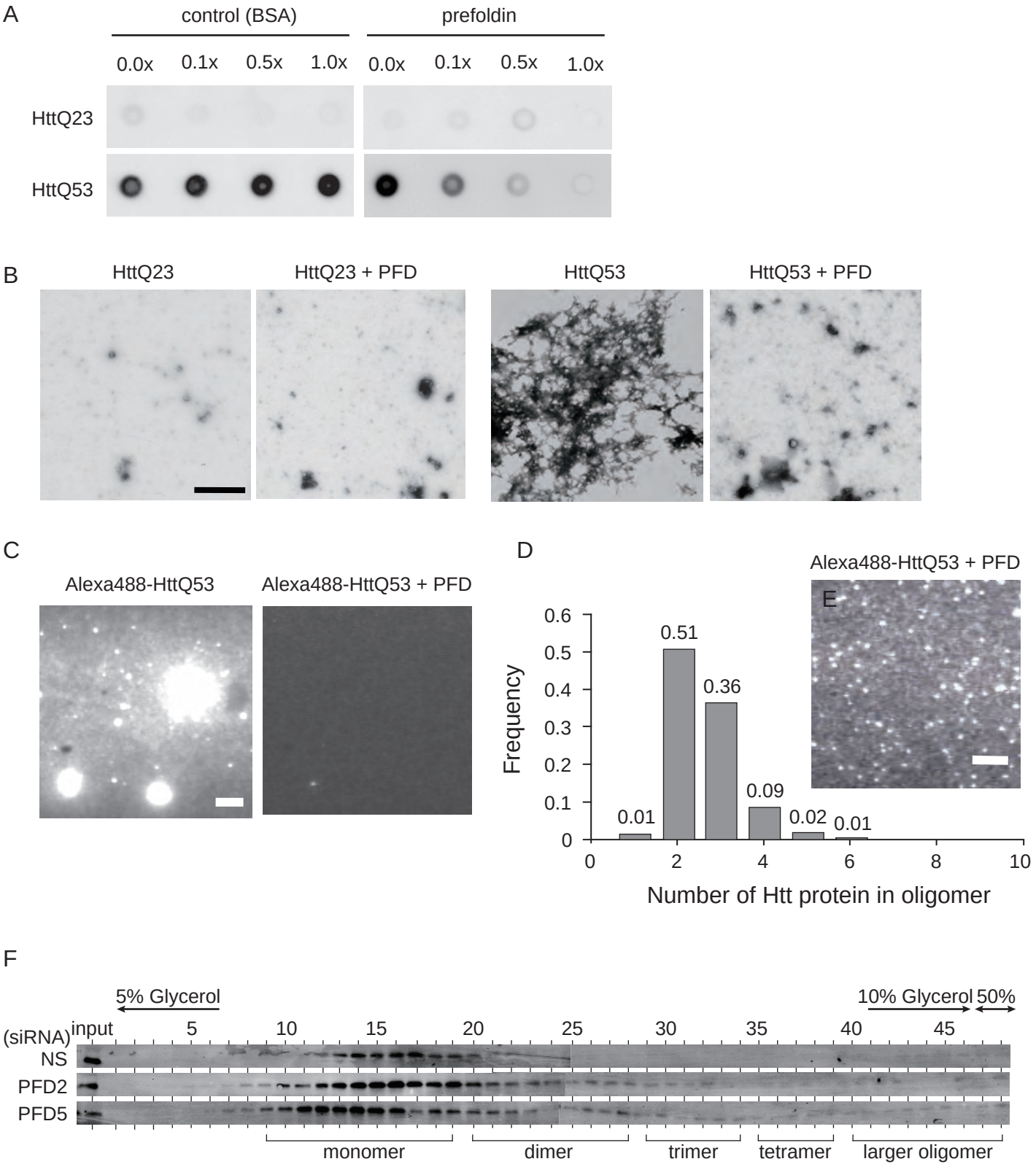
A
control (BSA)
prefoldin
0.0x
0.1x
0.5x
1.0x
0.0x
0.1x
0.5x
1.0x
HttQ23
HttQ53
B
HttQ23
HttQ23 + PFD
HttQ53
HttQ53 + PFD
C
Alexa488-HttQ53
Alexa488-HttQ53 + PFD
D
Alexa488-HttQ53 + PFD
E
Frequency
0.6
0.5
0.4
0.3
0.2
0.1
0
0.01
0.51
0.36
0.09
0.02
0.01
0
2
4
6
8
10
Number of Htt protein in oligomer
F
5% Glycerol
10% Glycerol
50%
(siRNA)
input
5
10
15
20
25
30
35
40
45
NS
PFD2
PFD5
monomer
dimer
trimer
tetramer
larger oligomer

Figure 7

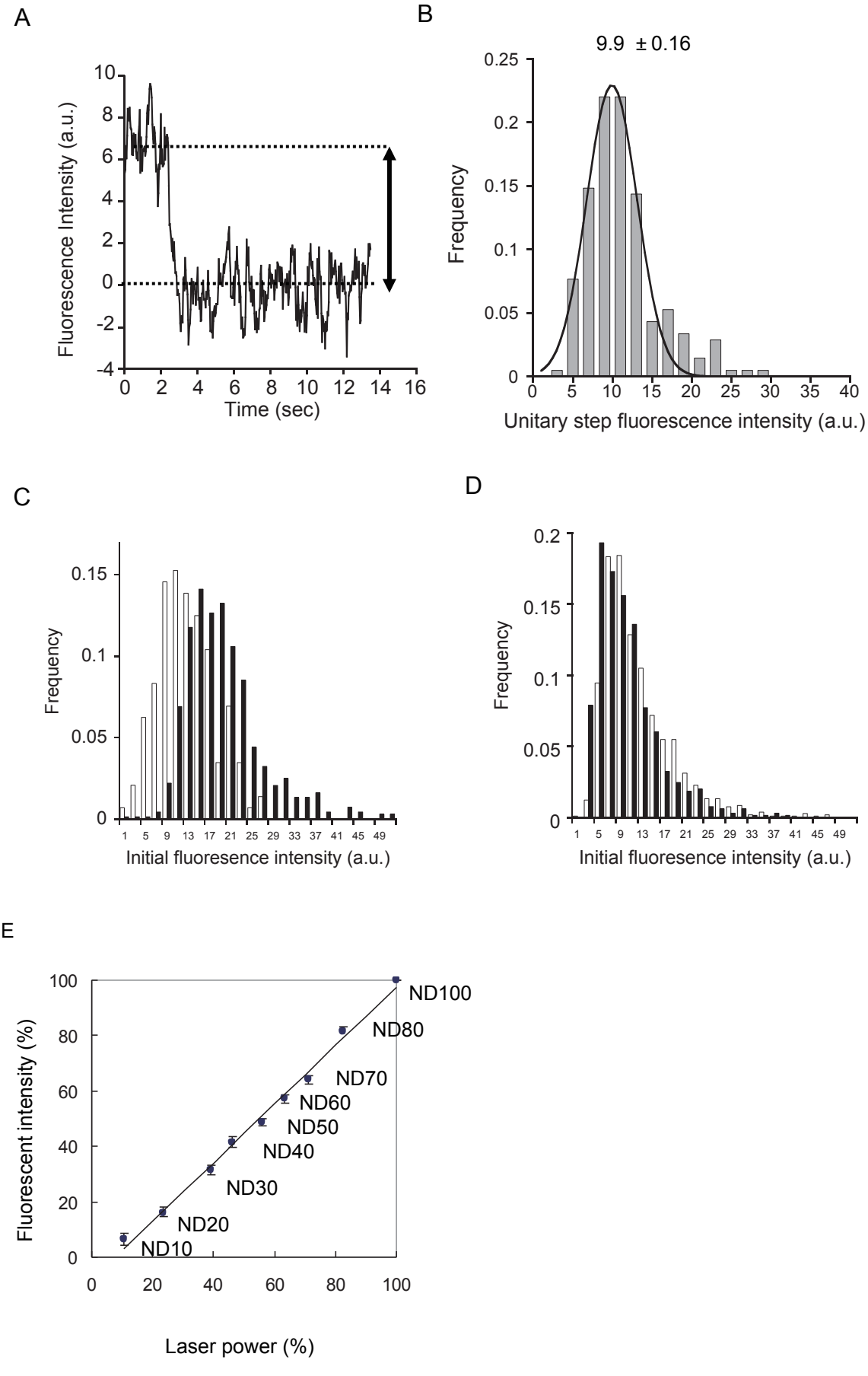
A
Fluorescence Intensity (a.u.)
Time (sec)
B
9.9 ± 0.16
Frequency
Unitary step fluorescence intensity (a.u.)
C
Frequency
Initial fluoresence intensity (a.u.)
D
Frequency
Initial fluoresence intensity (a.u.)
E
Fluorescent intensity (%)
Laser power (%)
ND10
ND20
ND30
ND40
ND50
ND60
ND70
ND80
ND100

Figure 8

A

A-a. Staurosporine

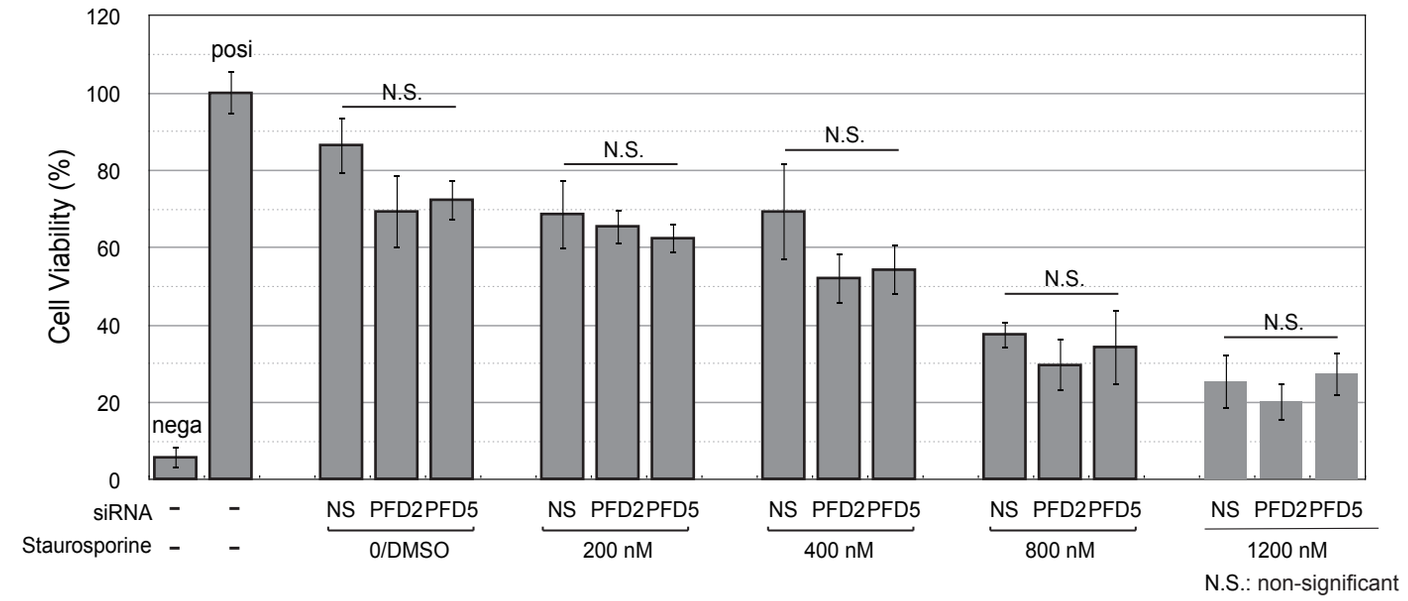

A-b. Thapsigargin

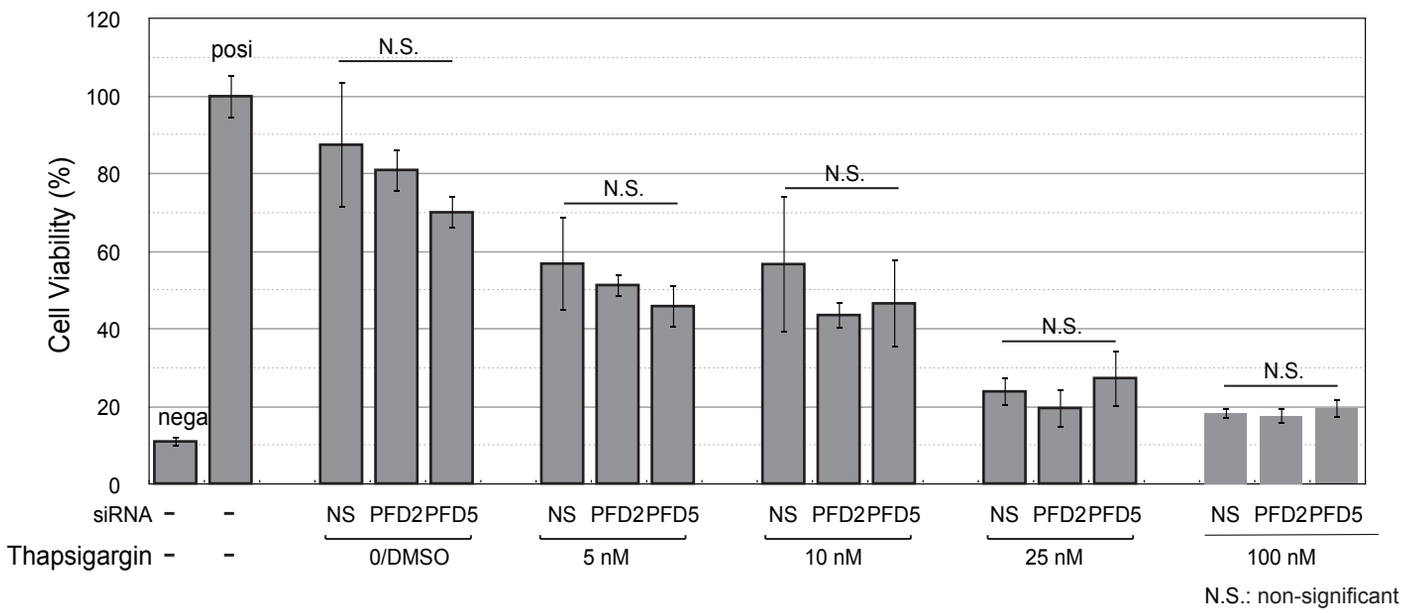

B

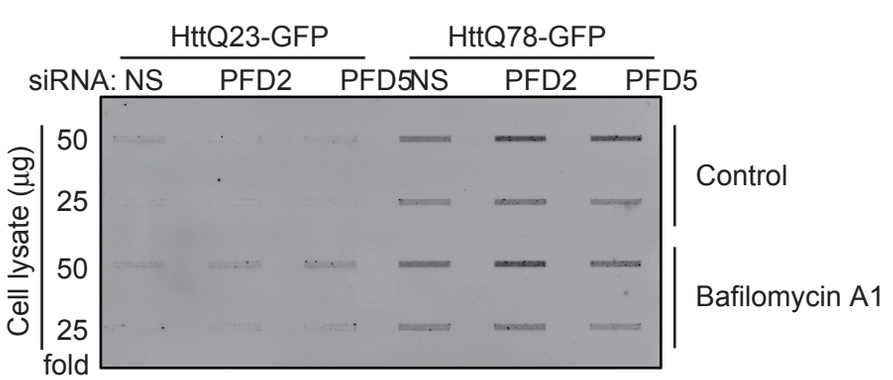

Figure 9

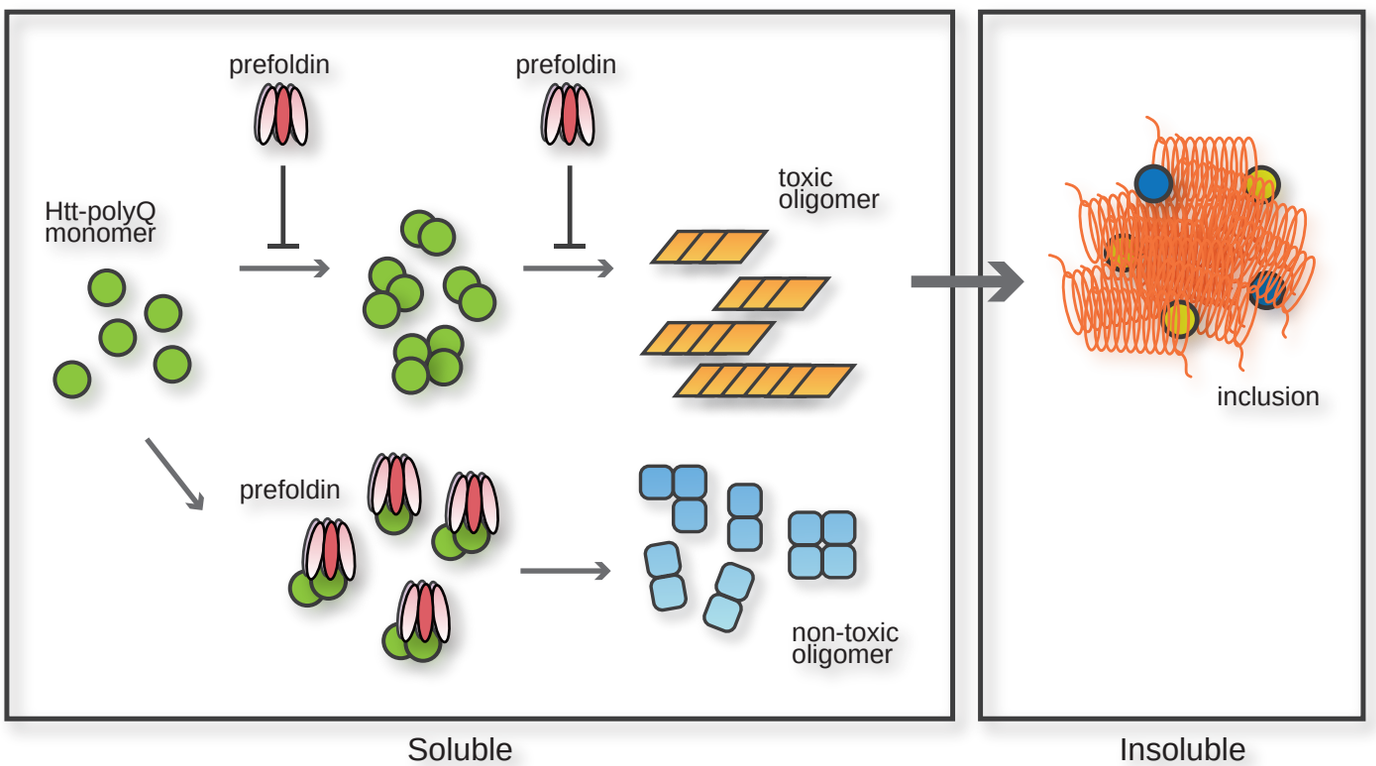
prefoldin
prefoldin
Htt-polyQ
monomer
toxic
oligomer
inclusion
prefoldin
non-toxic
oligomer
Soluble
Insoluble